

AI-NanoFunc workshops 2013

ABSTRACT BOOK

II. Nanomaterials for sustainable energy and protection of the environment

III. Advanced microstructural characterization of materials

Seville 1-2 July, 2013



Organized by



CSIC
CONSEJO SUPERIOR DE INVESTIGACIONES CIENTÍFICAS



Financed by



Table of Content

Welcome	iii
Venue	v
Program	vii
Scientific committee	xi
Local organizing committee	xiii
Abstracts Oral Presentations	
Session 1	3
Session 2	21
Abstracts Posters	
Poster Session	41

Nanomaterials for sustainable energy and protection of the environment
Advanced Microstructural Characterization of Nanomaterials
Sevilla 1-2 July 2013

Welcome

It is a great pleasure to welcome you to the 2013 AI-NanoFunc Workshops: **Workshop II - Nanomaterials for sustainable energy and protection of the environment**, and **Workshop III - Advanced microstructural characterization of nanomaterials**.

This book comprises the abstracts of the oral presentations and poster sessions of the workshops. During two days topics like hydrogen storage and production, nanomaterials for energy conversion and storage (i.e. more efficient photovoltaic, light emitting devices, etc), catalysis for environmental applications on workshop II and high resolution analytic microscopy: EDX, EELS, high resolution imaging: TEM, STEM and application to Functional Materials, on workshop III, will be under discussion.

Reflecting the main objectives and character of AI-NanoFunc project, these workshops aim to be an open discussion forum to bring together senior and young scientists. We would like to express our gratitude to all participants and invited speakers.

We are grateful to a number of organizations that funded or supported this event making it possible.

- EU FP7 capacities program REGPOT AI-NanoFunc
- Junta de Andalucía
- Instituto de Ciencia de Materiales de Sevilla CSIC-Universidad de Sevilla

Special thanks are given to those who help to prepare the 2013 AI-NanoFunc workshops, specially the members of the Scientific Committee and Local Organizing Committee.

Advanced Laboratory for the **NANO**-analysis of Novel **FUNC**tional Materials- Team

Asunción Fernández (Project Coordinator)

Vanda Godinho (Research manager)

Lucia Castillo (Secretary)

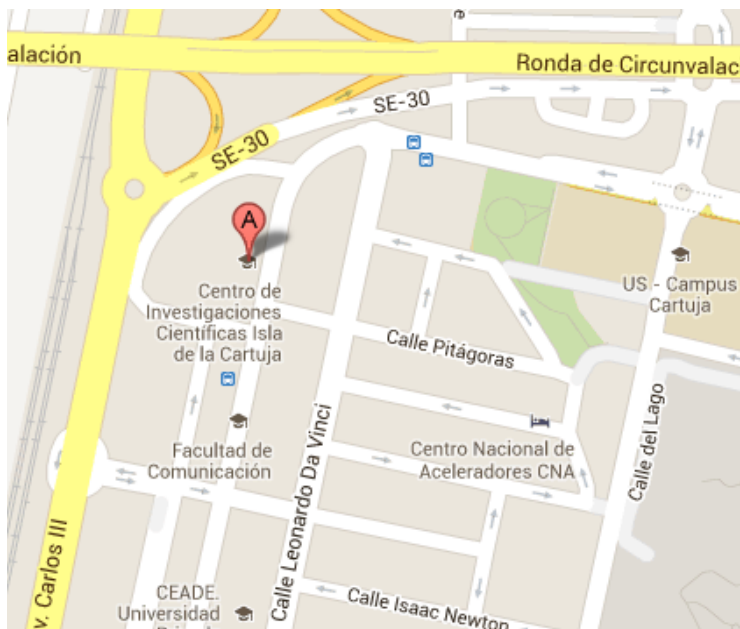
Rocío García (IT)

Nanomaterials for sustainable energy and protection of the environment
Advanced Microstructural Characterization of Nanomaterials
Sevilla 1-2 July 2013

Venue

The Material Science Institute will be hosting this event in joint collaboration with scientists of the network of collaborative centers in AI-NanoFunc.

The meeting will take place at the "CicCartuja", placed in 'La Isla de la Cartuja' in Seville.



Avda. Américo Vespucio 49
41092, Seville



cicCartuja

Nanomaterials for sustainable energy and protection of the environment
Advanced Microstructural Characterization of Nanomaterials
Sevilla 1-2 July 2013

Program

Monday 1st July

08:45-09:10	Registration
09:10-09:15	Welcome
Session 1	Advanced microstructural characterization of materials
09:15-09:55	Inv. S(TEM), a key tool for the design of novel ceria-zirconia materials with unconventional redox properties J. Calvino
09:55-10:00	questions
10:00-10:15	<i>Main contributions of TEM techniques to determine the nanoscale and chemical composition of the complex catalytic and magnetic systems: Co-B and Co-Ru-B</i> T.C. Rojas
10:15-10:20	questions
10:20-11:00	Inv. Recent advances in electron tomography Z. Saghi
11:00-11:05	questions
11:05-11:40	coffee break + poster session
11:40-11:55	<i>Advanced characterization of hybrid core@shell nanowires</i> M. Macias-Montero
11:55-12:00	questions
12:00-12:15	<i>Characterization of core@shell nanoparticles using advanced electron microscopy</i> B.R. Knappett
12:15-12:20	questions
12:20-13:00	Inv. High-resolution quantitative characterization of nanoparticles S. Lozano
13:00-13:05	questions
13:05-15:00	lunch
15:00-15:40	Inv. Get more out of EELS spectra: noise reduction, original background-removal functions and component analysis M. Duchamp
15:40-15:45	questions
15:45-16:00	<i>Study of deposition parameters on the microstructure of magnetron sputtered amorphous silicon coatings with closed porosity</i> J. Caballero-Hernandez
16:00-16:05	questions
16:05-17:30	coffee break + poster session

Nanomaterials for sustainable energy and protection of the environment
 Advanced Microstructural Characterization of Nanomaterials
 Sevilla 1-2 July 2013

Tuesday 2nd July

Session 2	Nanomaterials for sustainable energy and protection of the environment	
09:15-09:55	Inv. New approaches in heterogeneous photocatalysis for improved environmental applications	G. Colón
09:55-10:00	questions	
10:00-10:15	<i>Investigation of the catalyzed hydrolysis of ammonia borane in a continuous flow reactor for the hydrogen production at medium scale</i>	M. Paladini
10:15-10:20	questions	
10:20-10:35	<i>Chlorination of Toluene over Ionic Liquid grafted in Carbon Nanofiber</i>	A. Martinez
10:35-10:40	questions	
10:40-11:00	coffee break + poster session	
11:00-11:40	Inv. Plasmonics for beaming led emission	G. Lozano
11:40-11:45	questions	
11:45-12:00	<i>Resonant photocurrent generation in dye-sensitized periodically nanostructured photoconductors by optical field confinement effects</i>	M. Anaya
12:00-12:05	questions	
12:05-12:20	<i>Periodical structures to improve light harvesting in dye solar cell</i>	C. Lopez-Lopez
12:20-12:25	questions	
12:25-12:40	<i>Tailored luminescent emission of dyes embedded in porous resonators</i>	A. Jimenez
12:40-12:45	questions	
12:45-13:00	<i>Optofluidic Sensors based on nanoporous Bragg microcavities prepared by GLAD</i>	M. Oliva-Ramirez
13:00-13:05	questions	
13:05	Closure ceremony and farewell cocktail	

Poster session

P1	<i>BiPO₄ nanostars for luminescent applications</i> Criado Joaquín, Becerro Ana I., Cervera L., Fernández Camacho A. and Ocaña M.
P2	<i>Photocatalytic degradation of phenol over TiO₂. Effect of the TiO₂ surface treatment by fluorination or sulfation</i> J.J. Murcia Mesa, M.C. Hidalgo López and J.A. Navío Santos
P3	<i>An electron microscopy study of the nanostructure of collagen fibrils</i> S. Borrego-González, J. Becerra, A. Díaz-Cuenca
P4	<i>Fabrication and characterization of "small-molecules" core@shell nanowires</i> A. Nicolas Filippin, Maria Alcaire, Angel Barranco and Ana Borrás
P5	<i>Mean inner potential and skeletal density of zeolite MCM- 41 using TEM</i> Lionel C. Gontard, Rafal E. Dunin-Borkowski , T. Kasama
P6	<i>Remote plasma assisted glad deposition of oxide thin film nanostructures for optical and electronic applications</i> Julián Parra-Barranco, Victor Rico, Ana Borrás, Juan Pedro Espinós, Fabián Frutos, Agustín R. González-Elipe, Ángel Barranco
P7	<i>Quantification of InXGa1-xP Composition Modulation by Nanometric scale HAADF Simulations</i> C.E. Pastore, M. Gutiérrez, D. Araújo and E. Rodríguez-Messmer
P8	<i>Characterization of amorphous porous Silicon coatings by Transmission Electron Microscopy techniques</i> Roland Schierholz, Jaime Caballero, Vanda Godinho and Asunción Fernández
P9	<i>Damage induced by rare earth ion implantation in nitride semiconductors: a comparative study</i> B. Lacroix, S. Jublot-Leclerc, A. Declémy, K. Lorenz, and P. Ruterana
P10	<i>Relationship between morphological observations by transmission electron microscopy/X-Ray diffraction and physical properties of bio-based polymer/clay nanocomposites</i> Heriarivelo Risite, Omar Fassi-Fehri, Mostopha Bousmina, Khalil El Mabrouk

Nanomaterials for sustainable energy and protection of the environment
Advanced Microstructural Characterization of Nanomaterials
Sevilla 1-2 July 2013

Scientific committee

Agustín E. González Elipe

(Instituto de Ciencia de Materiales de Sevilla)

Alfonso Caballero Martínez

(Instituto de Ciencia de Materiales de Sevilla)

Asunción Fernández

(Instituto de Ciencia de Materiales de Sevilla)

Rafal E. Dunin-Borkowski

(Ernst Ruska Center for Microscopy and Spectroscopy with Electrons)

Hernán Míguez

(Instituto de Ciencia de Materiales de Sevilla)

Nanomaterials for sustainable energy and protection of the environment
Advanced Microstructural Characterization of Nanomaterials
Sevilla 1-2 July 2013

Local Organizing committee

Workshop II

Asunción Fernández

Gisela Arzac

Mariana Paladini

Dirk Hufschmidt

Carlos García

Workshop III

Vanda Godinho

Cristina Rojas

Lionel Gontard

Roland Schierholz

María del Carmen Jiménez de Haro

Local Secretariat

Vanda Godinho research.manager@al-nanofunc.eu

Lucía Castillo secretary@al-nanofunc.eu

Rocío García web@al-nanofunc.eu

Oral presentations

Session 1

Advanced microstructural characterization of materials

(S)TEM, a key tool for the design of novel ceria-zirconia materials with unconventional redox properties

D.C. Arias, M.P. Yeste, J.C. Hernández-Garrido, M.A. Muñoz, G. Blanco, J.M. Pintado, J.M. Rodríguez-Izquierdo, M.A. Cauqui, J.A. Pérez-Omil and J.J. Calvino*

Departamento de Ciencia de los Materiales e Ingeniería Metalúrgica y Química Inorgánica. Facultad de Ciencias. Universidad de Cádiz. Campus Río San Pedro, Puerto Real, 11510-Cádiz. Spain

*contact e-mail: jose.calvino@uca.es

Keywords: Ceria-Zirconia, Oxygen Storage Capacity, Low lanthanide content, STEM

Abstract

Starting from the knowledge gained, using a combined use of STEM chemical techniques, on the relationships between nanostructure and redox properties in the family of ceria-zirconia oxides(1,2), it has been possible to envisage a synthetic approach to prepare a new type of materials exhibiting highly improved reducibility at low temperatures (3,4).

These new materials feature a very low content of cerium in their formulation, just 15% molar, i.e. $\text{Ce}_{0.15}\text{Zr}_{0.85}\text{O}_2$, but provide Oxygen Storage Capacity (OSC) values much higher than those characteristic of conventional ceria-zirconia oxides containing much higher ceria amounts or even than those of other materials including noble metals in their formulation, Figure 1. The new materials allow a much more efficient usage of cerium in catalytic applications in which either oxygen exchange or hydrogen activation are a requisite.

STEM techniques have provided the structural clues to start to understand their macroscopic performance.

In this communication we will first review the contributions of STEM to understand the influence of high temperature redox pretreatments on the bulk and surface structure of conventional ceria-zirconia oxides (5) and, more particularly, on the occurrence of disorder-order transitions in this family of oxides.

This information will lead us to the key synthetic point of surface ceria-zirconia phases depicting novel and quite unconventional redox behavior. Thus, the synthesis and some redox properties of nanostructured 15% $\text{CeO}_2/\text{ZrO}_2$ and a 13% CeO_2/YSZ samples will be discussed, considering the large influence on their behavior or high temperature (severe oxidation, or SO, and severe reduction, or SR) redox aging treatments.

Finally we will focus on an in-depth analysis of the structure of these new phases by using a combination of a variety of STEM techniques and XPS (4). This structural information will be used to confirm the goals of the new synthetic approach for this family of materials and to rationalize their macroscopic performance.

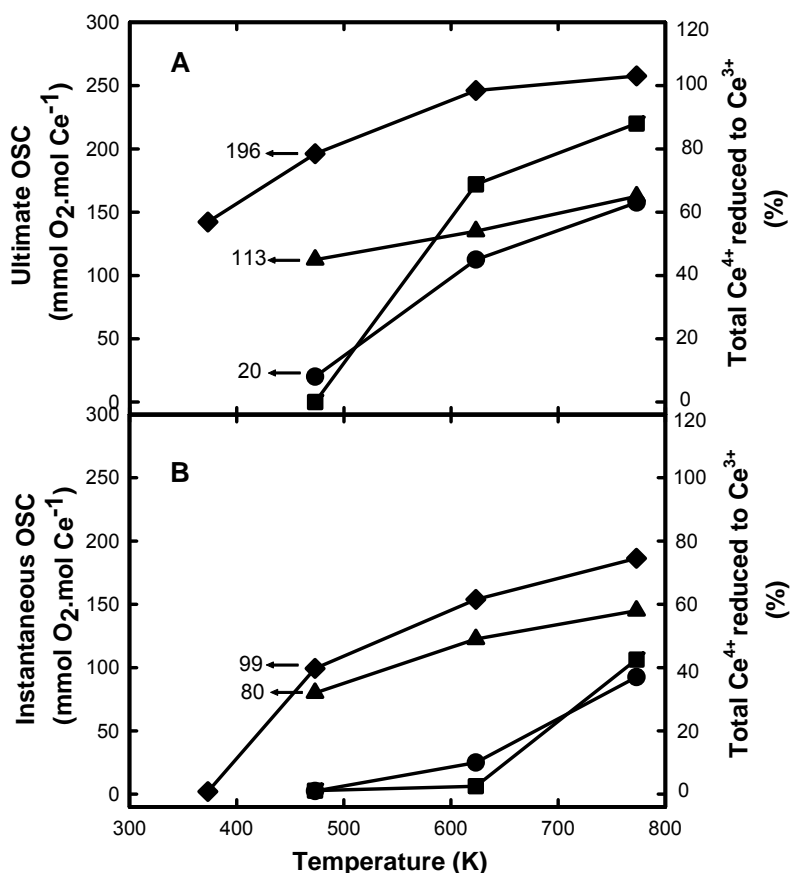


Figure 1 - Evolution with temperature of ultimate (A) and instantaneous (B) OSC values for: (■) a conventional Ce_{0.15}Zr_{0.85}O₂ oxide, (●) a conventional Ce_{0.62}Zr_{0.38}O₂ oxide, (▲) a Rh/Ce_{0.62}Zr_{0.38}O₂ catalyst, (◆) a novel 15% mol. CeO₂/YSZ material.

The whole set of results will clearly illustrate the role of atomic scale characterization techniques available at modern Scanning Transmission Electron Microscopes to unveil key aspects of materials functionalities and, from this basic knowledge, to devise new synthetic routes to obtain advanced materials.

References

- [1] M. P. Yeste, J. C. Hernandez, S. Trasobares, S. Bernal, G. Blanco, J. J. Calvino, J. A. Perez-Omil and J. M. Pintado, *Chem Mater*, 20 (2008) 5107-5113.
- [2] M. P. Yeste, J. C. Hernandez, S. Bernal, G. Blanco, J. J. Calvino, J. A. Perez-Omil and J. M. Pintado, *Chem Mater*, 18 (2006) 2750-2757
- [3] M. P. Yeste, J. J. Calvino, J. A. Pérez Omil, Juan Carlos Hernández Garrido, Ginesa Blanco Montilla, Diana Carolina Arias Duque, Patente nº 201200794
- [4] M. Pilar Yeste, Juan C. Hernández-Garrido, D. Carolina Arias, Ginesa Blanco, José M. Rodríguez-Izquierdo, José M. Pintado, Serafín Bernal, José A. Pérez-Omil and José J. Calvino, *J. Mater. Chem. A*, 2013, 1, 4836
- [5] M. Lopez-Haro, J. A. Perez-Omil, J. C. Hernandez-Garrido, S. Trasobares, A. B. Hungria, J. M. Cies, P. A. Midgley, P. Bayle-Guillemaud, A. Martinez-Arias, S. Bernal, J. J. Delgado and J. J. Calvino, *Chemcatchem*, 2011, 3, 1015-1027.

Main contributions of the TEM techniques to determine the nanostructure and chemical composition of the complex catalytic and magnetic systems: Co-B and Co-Ru-B.

G.M. Arzac^a, T.C. Rojas^{a*}, L. Cervera, A. Fernández^a

a. Instituto de Ciencia de Materiales de Sevilla (ICMS), CSIC-Univ. Sevilla. Américo Vespucio 49. Isla de la Cartuja. Seville. Spain.

*contact e-mail: tcrojas@icmse.csic.es

Keywords: HAADF-STEM, tomography, metal nanoparticles, amorphous Co-B.

Co-B and Co-Ru-B catalysts are widely used in the sodium borohydride hydrolysis to produce hydrogen for portable applications [1]. Co-B catalysts are easily prepared, cheap and efficient [2]. The addition of small amounts of Ru produces a significant enhancement in catalytic activity, the so called synergistic effect [3]. The magnetic behavior of a Co-B similar material had been also studied and published [4] but the magnetic performance when Ru is added has not been reported.

In a previous work a series of Co-Ru-B catalysts with variable Ru content were prepared by chemical methods, isolated and characterized. These materials result to be formed by spherical nanoparticles of around 20-40 nm, that contain small metal (Co and/or Ru) nanoparticles of around 2nm embedded in an amorphous matrix constituted by Co-Ru-B(O) phases, a veil/layer is covering this matrix, that in the case of the Co-Ru catalysts disappear when Ru content increases. This complex nanostructure, which has been understood after a full characterization, has allowed explaining the catalytic behavior and the synergetic effect [4-5]. In this work, an exhaustive study of these catalysts with different TEM (STEM-HAADF, Tomography) and associated spectroscopic techniques, using different lateral resolution is presented. Aspects such as homogeneity and possible formation of Co-Ru solid solution are analyzed and discussed. This study gives new data about the structure, the 3D morphology and composition of the samples, very useful to better explain the catalytic performance and to understand the singular magnetic behavior. Changes in the magnetic properties when the Ru is added have been found, and they are analyzed and explained taking into account the changes in the chemical composition and the nanostructure.

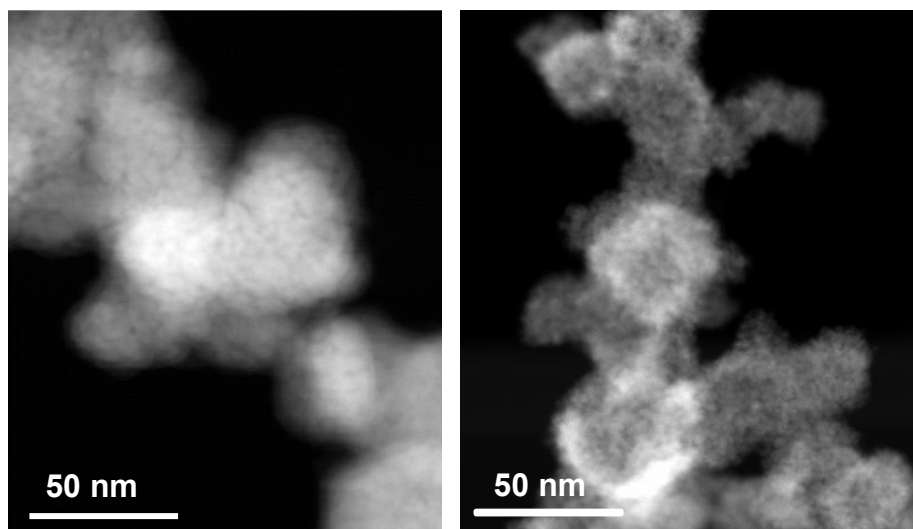


Figure. HAADF-STEM or Z-Contrast images of samples Co_B (left) and CoRuB (right).

References

- [1] U.B Demirci, O.Akdim, J. Andrieux, J. Hannauer, R. Chamoun, P.Miele, *Fuel Cells*, 2010, **3**, 335-350. References therein
- [2] U.B. Demirci, P.Miele, *Phys. Chem. Chem Phys*, 2010, **12**, 14665-14651.
- [3] J.H. Park, P. Shakkthivel, H.J. Kim, M.K. Han, J.H. Jang, Y.R. Kim, H.S. Kim, Y.G Shul, *Int J. Hydrogen Energy*, 2008, **33**, 1845-1852.
- [4] Ana B. Dávila-Ibáñez, Jose L. Legido-Soto, Jose Rivas and Verónica Salgueirino. *Phys. Chem. Chem Phys.*, **13**, 20146-20154, (2011).
- [5] G.M. Arzac, T.C. Rojas and A. Fernandez. *ChemCatChem* **3**, 1-10, (2011).
- [6] G.M. Arzac, T.C. Rojas, A. Fernández. *Applied catalyst B: environmental* **128**, 39-47 (2012).

Recent advances in Electron Tomography

Zineb Saghi^{a*}, Rowan Leary^a and Paul A. Midgley^a

^a *Department of Materials Science and Metallurgy, University of Cambridge, Pembroke Street, Cambridge, CB2 3QZ, UK*

*contact e-mail: zs256@cam.ac.uk

Keywords: electron tomography, STEM, 3D imaging, aberration correction.

Abstract

Electron tomography (ET) has become a well-established tool for the 3D characterization of both organic and inorganic materials [1]. In a typical ET experiment, a series of projections is recorded at different tilt angles, and a reconstruction algorithm is employed to generate the 3D volume. While an ET reconstruction can routinely reach nanometer resolution, achieving truly quantitative volumes is still a challenging task. This is due to the limited tilt range available in the microscope and the related artefacts such as distorted features and anisotropic loss of resolution. In this talk, we will highlight the progress made toward improving the fidelity of the reconstruction with the design of sophisticated tomography holders, acquisition schemes and reconstruction methods. More specifically, we will present the latest algorithmic developments with emphasis on the recent introduction of compressed sensing ET (CS-ET) [2]. By using the prior knowledge that the signal is sparse or compressible in a chosen transform domain (e.g. pixel or gradient domains), CS-ET employs a non-linear optimization algorithm to recover the sparsest solution consistent with the acquired projections. Applying CS-ET to iron oxide nanoparticles with reactive concavities (figure 1), we will show that the technique is capable of providing high-fidelity reconstructions from severely undersampled tilt series, using the prior knowledge that the nanoparticles are sparse both in the pixel representation (i.e. few pixels have nonzero values) and in the total variation domain (i.e. the object has sharp boundaries and uniform density). Figure 1 shows that quantitative information can be extracted reliably from reconstructions obtained with only nine projections, suggesting that there is a clear potential for the study of electron beam sensitive specimens, as well as use in conjunction with in-situ and time-resolved techniques.

Another challenge is extending the resolution of the technique to the atomic level. The recent development of aberration-corrected TEM and STEM has opened up new opportunities for imaging at unprecedented resolution with quantitative and directly interpretable data. The current progress made in pushing the 3D capabilities of the technique to the atomic level will be presented and novel approaches will be discussed, including the quantification

of 2D images, focal series reconstruction, 3D depth sectioning, and tilt series reconstruction. We believe that 3D atomic imaging will be successful across a range of materials and devices only if we use a combination of novel imaging modes, dedicated hardware, and reconstruction algorithms specifically designed for undersampled data sets.

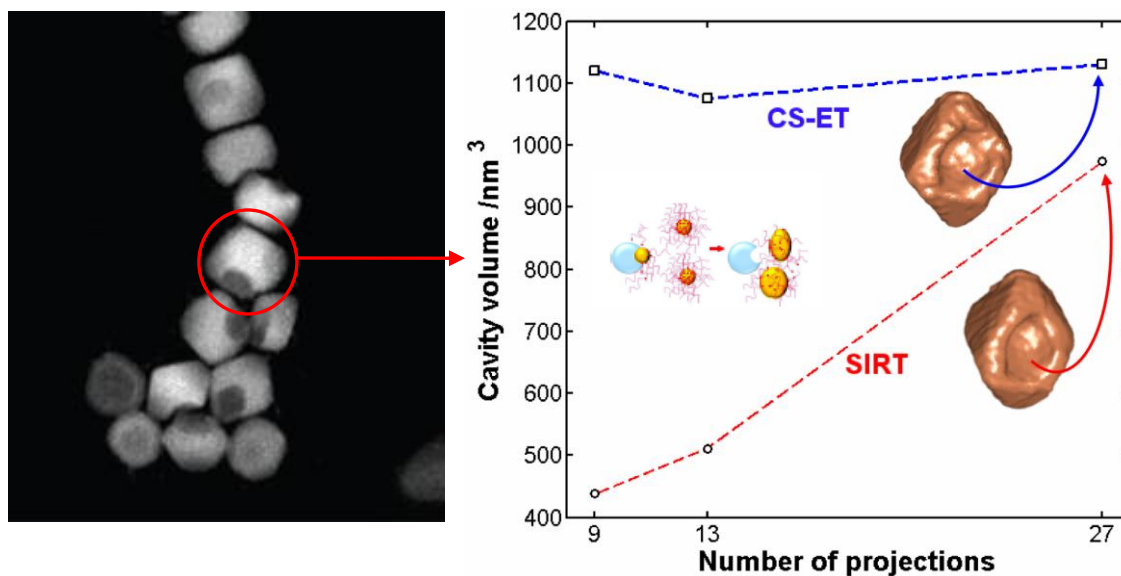


Figure 1 –Illustration of the robustness of CS-ET to undersampled data. Estimation of the concavity volume of the selected iron oxide nanoparticle (*circled in red*), using CS-ET and SIRT reconstructions obtained with 9, 13, and 27 projections. From [2].

References

- [1] P A Midgley et al, *Chemical Society Reviews*, **36** (2007), 1477.
- [2] Z Saghi et al, *Nano Letters* **11** (2011), 4666.

Advanced characterization of hybrid core@shell nanowires

M. Macias-Montero^{*,a}, Z. Saghi^b, A. N. Filippin, A. Barranco, J. P. Espinos, A. R. Gonzalez-Elipe and A. Borrás^a

^a *Nanotechnology on Surfaces Laboratory, Materials Science Institute of Seville (ICMSE), CSIC—University of Seville, C/Americo Vesputio 49, E-41092 Seville, Spain*

^b *Department of Materials Science and Metallurgy, University of Cambridge, Pembroke Street, Cambridge CB2 3QZ, UK*

*contact e-mail: manuel.macias@icmse.csic.es

Keywords: HAADF-STEM, hybrid nanostructures, core@shell nanocrystalline, 1D optical waveguiding, superhydrophobic-superhydrophilic transformation.

Abstract

In this work we aim to the advanced characterization of multifunctional organic/inorganic supported NWs fabricated by a novel full-vacuum methodology. These nanostructures consist of single crystal organic NWs conformally covered by an inorganic shell. Organic counterpart formation is based on self-assembly by pi-stacking of small molecules [1] meanwhile the inorganic shells are single or multilayer systems combining two well-known wide band gap semiconductors, ZnO and TiO₂ [2]. Figure 1 shows an example of this type of heterostructure formed by an inner single crystal organic nanowire as core completely surrounded by a ZnO shell. ZnO and TiO₂ in the form of nanostructures present important applications in fields ranging from nanosensors to solar light harvesting, including their outstanding performance as active photonic materials. Thus, we expect these new nanostructures to be of interest in different applications such as multisensors, solar cells and photonic nano-components. The performance of the organic@inorganic NWs in the aforementioned topics depends greatly on i) the inorganic semiconductor microstructure (columnar u homogeneous, type and connectivity of the porous structure, etc.) and structure (controlling for instance the electrical and optical properties), ii) crystal structure of the organic nanowire forming the core of the heterostructures and iii) interface between the organic core and the inorganic shell. Thus, following the lead of our communication in the first edition of this workshop and the description of the full vacuum approach to the growth of the hybrid nanowires in ref. [3], we now present the characterization of the hybrid organic/inorganic core/shell nanowires by several TEM techniques in the framework of an AL-Nanofunc PhD. student short-stay. We have taken advantage of the use of high angle annular dark field scanning transmission electron microscopy (HAADF-STEM) to perform a 3D reconstruction of these 1D nanostructures [Fig. 1 b]. These results along with the HRTEM performed in Titan3 G2 60-300 TEM and SEM characterization of the materials provide a full description of the hybrid nanowire core/shell structures, microstructures and compositions.

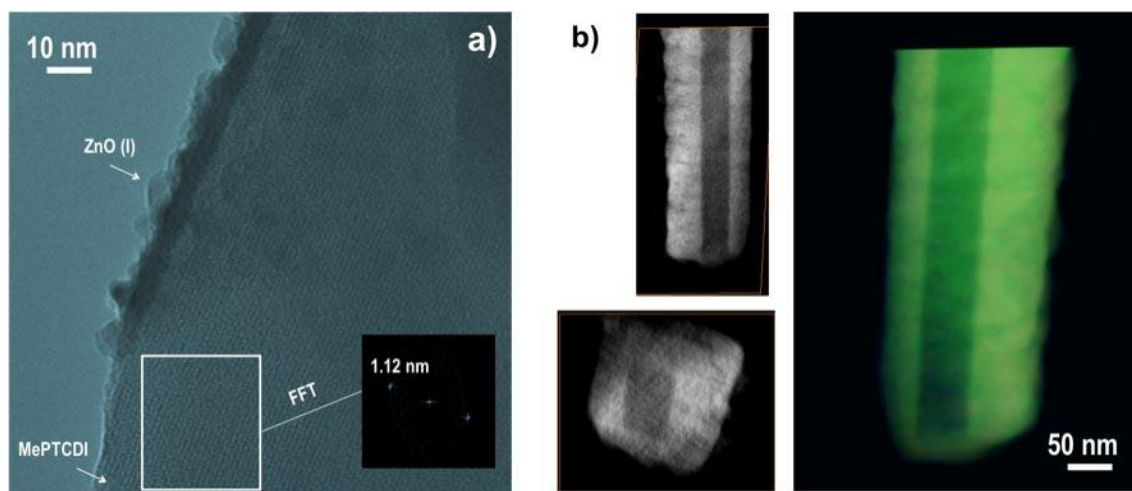


Figure 1 – a) HRTEM micrograph of a MePTCDI/ZnO hybrid nanowire, highlighting the unaltered organic crystal structure; b) HAADF-STEM 3D reconstruction snapshots of a ZnPc/SiO₂ hybrid nanowire.

References

- [1] A. Borrás, O. Groning, M. Aguirre, F. Gramm, P. Groning *Langmuir* **26** (2010), 5763.
- [2] P. Romero-Gómez, J. Toudert, J.R. Sánchez-Valencia, A. Borrás, A. Barranco, A.R. González-Elípe *Journal of Physical Chemistry C* **114**, 20932–20940 (2010); A. Borrás, J. Cotrino, A.R. González-Elípe *Journal of the Electrochemical Society* **154**, p152-p157 (2007).
- [3] M. Macias-Montero, A. N. Filippin, Z. Saghi, F. J. Aparicio, A. Barranco, J. P. Espinos, F. Frutos, A. R. Gonzalez-Elípe and A. Borrás *Advanced Functional Materials* DOI: 10.1002/adfm.201203390

Characterisation of Co@Fe₃O₄ core@shell nanoparticles using advanced electron microscopy

Benjamin R. Knappett,^a Pavel Abdulkin,^a Emilie Ringe,^b David A. Jefferson,^a Sergio Lozano-Perez,^{*c} T. Cristina Rojas,^d Asunción Fernández^{*d} and Andrew E. H. Wheatley^{*a}

^a Department of Chemistry, University of Cambridge, Lensfield Road, Cambridge, CB2 1EW, UK

^b Department of Materials Science and Metallurgy, University of Cambridge, Pembroke Street, Cambridge, CB2 3QZ.

^c Department of Materials, University of Oxford, Parks Road, Oxford, OX1 3PH, UK

^d Ciencia de Materiales de Sevilla CSIC - Univ. Sevilla Avda. Américo, Vespucio nr. 49, CIC Cartuja 41092-Sevilla, Spain

*contact e-mail: aehw2@cam.ac.uk

Keywords: Core, shell, magnetic, nanoparticle, EELS

Abstract

In recent years there has been significant interest in the synthesis of bimetallic or metal oxide nanoparticles (NPs) with a core@shell structure,¹ as they have been suggested for a number of applications such as magnetic separation, catalysis,^{8,9} targeted drug delivery,¹⁰ and magnetic hyperthermia.² Core@shell structures are often proposed in the literature, albeit evidence of successful synthesis is commonly based on bulk analysis techniques, or on the increase in mean size between the pre-formed seed (core) NPs and the coated product.

In order to identify the true structure of individual particles one must rely on more sophisticated approaches, such as spatially resolved micro-analytical methods.

To this end, cobalt NPs were synthesised via the thermal decomposition of Co₂(CO)₈ and were coated with iron oxide using Fe(CO)₅.³ While previous work focused on the subsequent thermal alloying of these nanoparticles, this study fully elucidates their composition and core@shell structure. State-of-the-art electron microscopy and statistical data processing enabled chemical mapping of individual particles through the acquisition of energy-filtered transmission electron microscopy (EFTEM) images (Figure 1) and detailed electron energy loss spectroscopy (EELS) analysis (Figure 2). Multivariate statistical analysis (MSA) has been used to greatly improve the quality of elemental mapping data from the core@shell NPs. Results from a combination of spatially resolved microanalysis reveal the shell as Fe₃O₄ and show that the core is composed of oxidatively stable, metallic Co. For the first time, a region of lower atom density between the particle core and shell has been observed, and this has been identified as a trapped carbon residue attributable to the organic capping agents present in the initial Co NP synthesis.

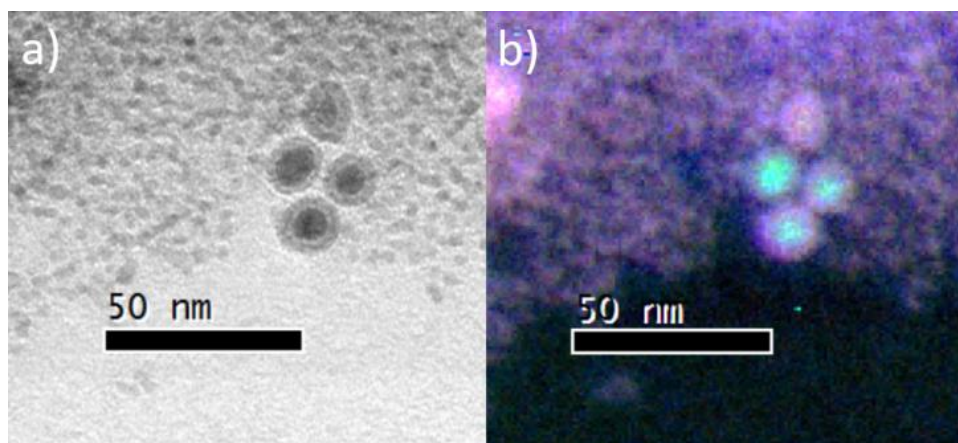


Figure 1 – EFTEM images of Co@Fe₃O₄ core@shell particles. a) bright field TEM image; b) an overlay of Co (green), Fe (pink) and O (blue) compositional maps.

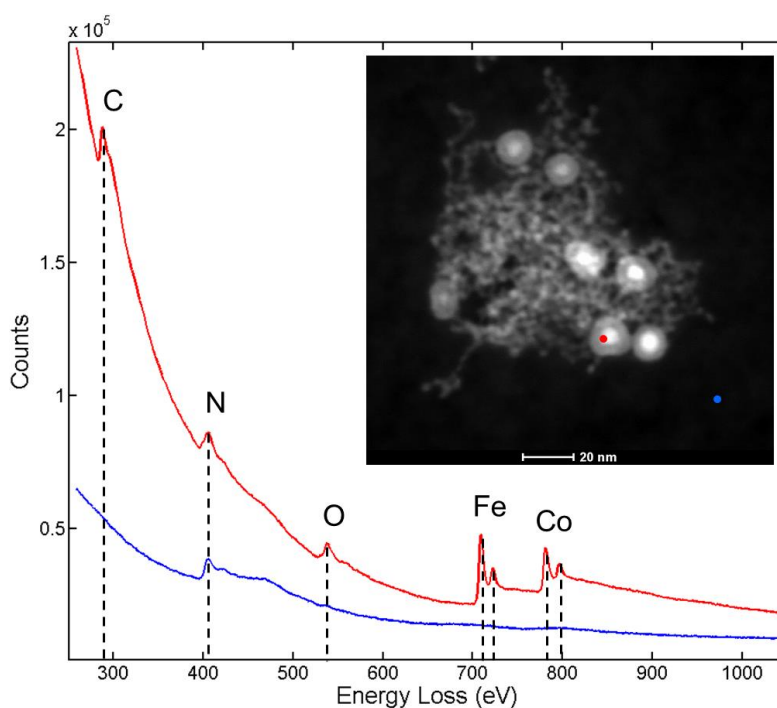


Figure 11 – EELS point spectra (from a plasma cleaned sample) of the Si₃N₄ thin film coating the microscope grid (blue lower line) and of the interface of the core and shell of a core@shell particle (red top line). It can be clearly seen that carbon is present within the particle despite plasma cleaning.

References

- [1] J. Gallo, I. García, D. Padro, B. Arnáiz, and S. Penadés, *J. Mater. Chem.*, **20** (2010) 10010.
- [2] C. Altavilla and E. Ciliberto, *Inorganic Nanoparticles: Synthesis, Applications and Perspectives*, CRC Press, 1st Ed., 2011.
- [3] S. Sun, C. Wang, S. Peng, and L.-M. Lacroix, *Nano Res.* **2** (2009) 380–385.

High-resolution quantitative characterization of nanoparticles

Sergio Lozano-Perez^{*a}, Kate MacArthur^a, Haibo E^a, Benjamin R. Knappett^b, Pavel Abdulkin^b, Andrew E. H. Wheatley^b, Cristina Rojas-Ruiz^c and Asuncion Fernandez^c

^a Department of Materials, University of Oxford, Parks Rd, OX1 3PH Oxford, UK

^b Department of Chemistry, University of Cambridge, Lensfield Rd, Cambridge, CB2 1EW, UK

^c Ciencia de Materiales de Sevilla CSIC – Univ. Sevilla Avda. Americo, Vesputio 49, CIC Cartuja, 41092-Sevilla, Spain

* Sergio.lozano-perez@materials.ox.ac.uk

Keywords: HREM, HAADF, quantitative, EDX, core-shell

Abstract

Nanoparticles have demonstrated immense promise for hydrogen fuel cell applications, drug delivery or magnetic separation. However, due to their multi-component nature, small size and reactivity, they are challenging to characterize at the nano-scale. Several examples of a high-resolution quantitative characterization, including bimetallic and core-shell nanoparticles will be presented.

Pt-Pd bimetallic particles not only provide a mass reduction of platinum but also a significant increase in the catalytic activity. In order to understand these systems further it is necessary to understand their 3-dimensional structure and composition at the atomic scale. Reconstructing the 3-dimensional structure of a particle normally requires taking a series of images at different tilts to combine information; this is not possible with such beam sensitive materials where the particle is likely to reconstruct under the beam so multiple images is often not possible. In Oxford, we have applied a new technique, the scattering cross-section, which uses the composition contrast information of high angle annular dark-field (HAADF) scanning transmission electron microscopy (STEM) for atom counting and particle reconstruction from a single image (see Figure 1). The potential of this approach will be explained.

Core-shell Cobalt-based nanoparticles synthesised via the thermal decomposition of $\text{Co}_2(\text{CO})_8$ and coated in iron oxide using $\text{Fe}(\text{CO})_5$ have also been characterized. A detailed summary of the results will be provided in the talk by Ben Knappett. Here, we'll focus on the analysis of the suitability of EELS and EDX for this characterization and a discussion of how the limits of these techniques can be pushed further.

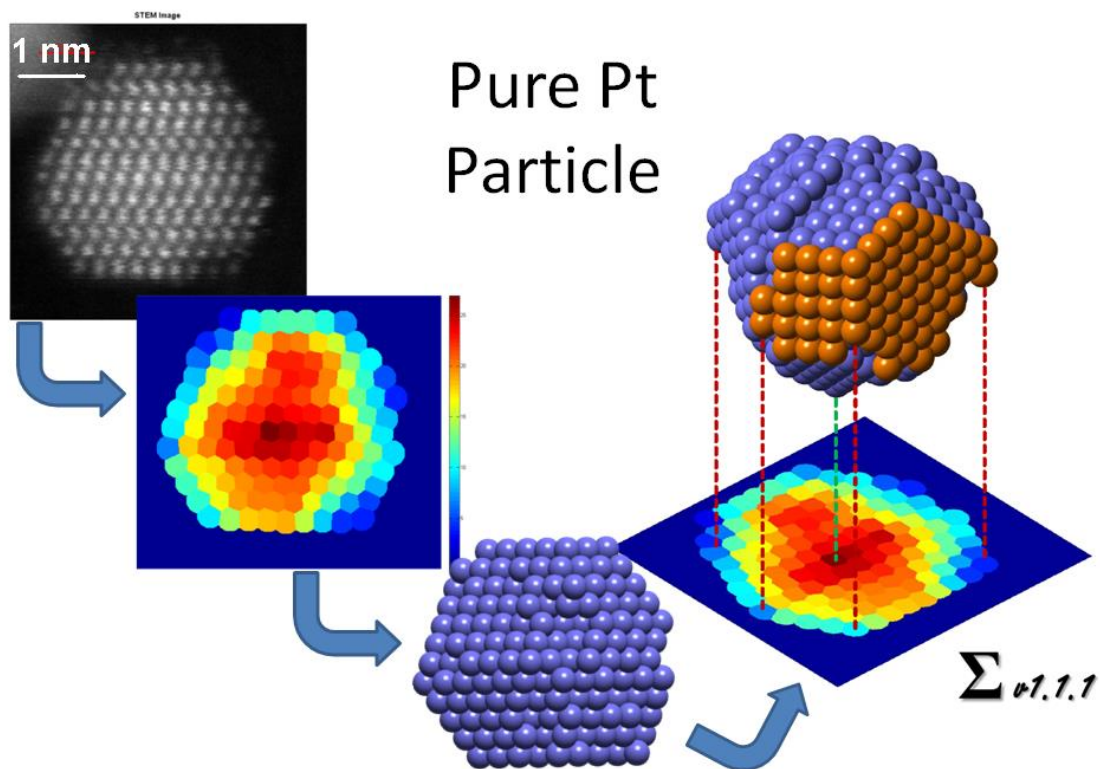


Figure 1 – Procedure followed to extract cross-section values from HAADF image of a pure Pt nanoparticle. The data is calibrated and used to propose a 3D model of the particle that it is then compared with the experimental data.

References

- [1] E, H.; Nellist, P. D.; D'Alfonso, A. J.; et al., *Journal of Physics Conference Series* **371** (2012), 012027.
- [2] Knappett, B.R., Abdulkin, P., Ring, E. et al., *Nanoscale*, **5** (2013), 5765.

Get more out of EELS spectra: noise reduction, original background-removal functions and component analysis

Martial Duchamp*, Chris B. Boothroyd, András Kovács and Rafal E. Dunin-Borkowski

Ernst Ruska-Centre for Microscopy and Spectroscopy with Electrons (ER-C)
and Peter Grünberg Institute (PGI), Forschungszentrum Jülich, D-52425 Jülich,
Germany

*contact e-mail: martial.duchamp@gmail.com

Abstract

Thin films of hydrogenated amorphous Si (a-Si:H) are used as active absorber layers in solar cells deposited on steel foil by roll-to-roll processing [1]. In order to improve the efficiency of such solar cells, the nature of the defects that act as charge recombination centres and decrease the internal electric field in the active Si layer needs to be understood. We have used electron energy-loss spectroscopy (EELS) in the transmission electron microscope (TEM) to study *n-i-p* thin film Si solar cells grown on steel foil or glass substrates. For a solar cell in which an intrinsic a-Si:H layer is sandwiched between 10-nm-thick n-doped and p-doped a-Si:H layers, we assess whether core-loss EELS can be used to measure the diffusion of B from the *p* to the *i* layer. The difficulty of such measurements results in part from the fact that the energy-loss near-edge structure from the Si L edge interferes with the B K edge at 188 eV. In addition, the Si L_{2,3} edge cross-section is five times larger than that of the B K edge. We use dedicated EEL spectrum acquisition and fitting procedures to reduce the detector noise and to separate the B K edge contribution from the Si fine structure for B concentrations as low as 1 at. %. We compare the shape of the measured B K edge with real space *ab initio* multiple scattering calculations and show that it is possible to separate the weak B K edge peak from the much stronger Si L edge fine structure by using log-normal fitting functions. Line profiles of B concentrations measured using core-loss EELS are compared with secondary ion mass spectrometry (SIMS) profiles recorded using two different ions energies from the same sample. We also assess whether changes in volume plasmon energy can be related to the electrically active B concentration and/or to the density of the material and whether variations of the volume plasmon line-width can be correlated with differences in the scattering of valence electrons in differently doped a-Si:H layers [1, 2].

In a separate experiment, we study the chemical compositions of defective regions in thin film Si solar cells using energy-dispersive X-ray spectroscopy

and EELS in the scanning TEM. We use nanometer-resolved chemical analysis to reveal the presence of ZnO in micrometer-long defective regions. We apply an unmixing algorithm to the EELS measurements to determine the chemical compositions of the defective regions objectively, without introducing artefacts from fitting procedures. The resulting spectral components, which are inferred to correspond to Si, ZnO and SiO₂ + C signals. The results obtained using this spectral decomposition procedure indicate that the defective regions in the Si layer are filled with ZnO, which diffuses along voids that propagate from the bottom of the absorber layer up to the top ZnO contact [3].

References

- [1] C. B. Boothroyd, K. Sato and K. Yamada, *Proceedings of the XII International Congress on Electron Microscopy, edited by L. D. Peachey and D. B. Williams, Seattle, Washington, 12-18 August 1990, (San Francisco Press, San Francisco, 1990), p. 80*
- [2] M. Duchamp, C. B. Boothroyd, M. S. Moreno, B. B. van Aken, W. J. Soppe and R. E. Dunin-Borkowski, *Journal of Applied Physics* **113** (2013), 093513
- [3] M. Duchamp, M. Lachmann, C. B. Boothroyd, A. Kovács, F.-J. Haug, C. Ballif and R. E. Dunin-Borkowski, *Applied Physics Letters*, **102** (2013), 133902

Study of deposition parameters on the microstructure of magnetron sputtered amorphous silicon coatings with closed porosity

J. Caballero-Hernández^{a*}, R. Schierholz^a, V. Godinho^a, M. Duchamp^b, R. Dunin-Borkowski^b, A. Fernández^a

^a *Instituto de Ciencia de Materiales de Sevilla, CSIC-Uni, Sevilla, Sevilla, Spain*

^b *Ernst Ruska-Centre for Microscopy and Spectroscopy with Electrons, Forschungszentrum Jülich, D-52425 Jülich, Germany*

*contact e-mail: jaime.caballero@icmse.csic.es

Keywords: silicon porous coating, oblique angle deposition (OAD), closed porosity

Abstract

In last years, the research in porous silicon has become a growing field due to the many possible applications such as solar cells [1], optoelectronics [2] and photonic devices [3].

We recently presented a new bottom up method for the production of amorphous porous silicon coatings with closed porosity by magnetron sputtering [4]. The advantages of this approach in relation to the traditional electrochemical methods are the possibility to produce coatings with closed porosity by depositing directly on large areas and different kinds of substrates like glass or even sensible and flexible substrates like polymers [4], the close porosity avoids the aging drawbacks due to exposition to air, typical of open porosity obtained by electrochemical methods. In addition, the refractive index of the coatings can be easily changed just by changing the sputtering gas: coatings with closed porosity are obtained using helium as sputtering gas and denser coatings can be obtained with argon, which can be very interesting for the development of Bragg mirrors and optical cavities [4] by depositing multilayers of both materials. Our preliminary studies indicate that the closed pores are filled with the deposition gas [4, 5] (see also "Characterization of amorphous porous Silicon coatings by Transmission Electron Microscopy techniques", R. Schierholz et al presented to this conference).

However, understanding the growth mechanism and the influence of the deposition parameters on the microstructure of these new porous silicon coatings is necessary. In this work we present a systematic study by electron microscopy of closed porous silicon coatings deposited by magnetron sputtering under different deposition conditions. The influence of vapor incidence angle ($\alpha=0^\circ$ and 30°) on the pore alignment was investigated using the two setups, sketched in the figure 1(a and b); a clear orientation of the pores on the direction of vapor flux was observed [4](figure 1 c and d).

Oblique angle deposition (OAD) of porous silicon coatings was further explored in this work. The influence of pressure on the growth of columnar coatings has been widely investigated by other authors [6, 7]. A similar behavior was found for the pore orientation; increasing pressure results in a decreased angle for the pore alignment (see figure 1 e and f). The increased pressure results also in a narrower pore size as

observed in the insets of figure 1 e and f. Pore sizes can also be controlled by changing the power supplied to the magnetron (figure 1 g and h).

Other important parameters on the shadowing effects characteristic of OAD as substrate temperature [7, 8] and substrate bias [9, 10] were also investigated.

References

- [1] A. Ramizy, Z. Hassan, K. Omar, Y. Al-Domi, M.A. Mahdi, *Applied Surface Science*, **257** (2011) , 6112.
- [2] D. Abidi, S.Romdhane, A. Brunet-Burneau, J.L. Fave, *European Physical Journal Applied Physics*, **45** (2009), 10601.
- [3] R.S. Dubey, D.K. Gautam, *Optik*, **122** (2011), 494.
- [4] V. Godinho, J. Caballero-Hernández, D. Jamon, T.C. Rojas, R. Schierholz, J. García-López, F.J. Ferrer, A. Fernández, A new bottom-up methodology to produce silicon layers with a closed porosity nanostructure and reduced refractive index, *accepted to Nanotechnology*.
- [5] V. Godinho, T.C. Rojas, A.Fernandez, *Microporous and Mesoporous Materials* **149** (2012) 142-146
- [6] J. Lintymer, J. Gavaille, N. Martin, J. Takadoum, *Surface and Coatings Technology* **174 –175** (2003) 316–323.
- [7] R. Alvarez, J.M. García-Martín, M. Macías-Montero, L. Gonzalez-Garcia, J.C. González, V. Rico, J. Perlich, J. Cotrino A.R. González-Elipe, A. Palmero, *Nanotechnology* **24** (2013) 045604
- [8] J.A.Thornton, *Annual Review of Materials Science* **7** (1977) 239-260
- [9] S. Mahieu, P. Ghekiere, D. Depla, R. De Gryse, *Thin Solid Films* **515** (2006) 1229-1249
- [10] A. Anders, *Thin Solid Films* **518** (2010) 4087-4090

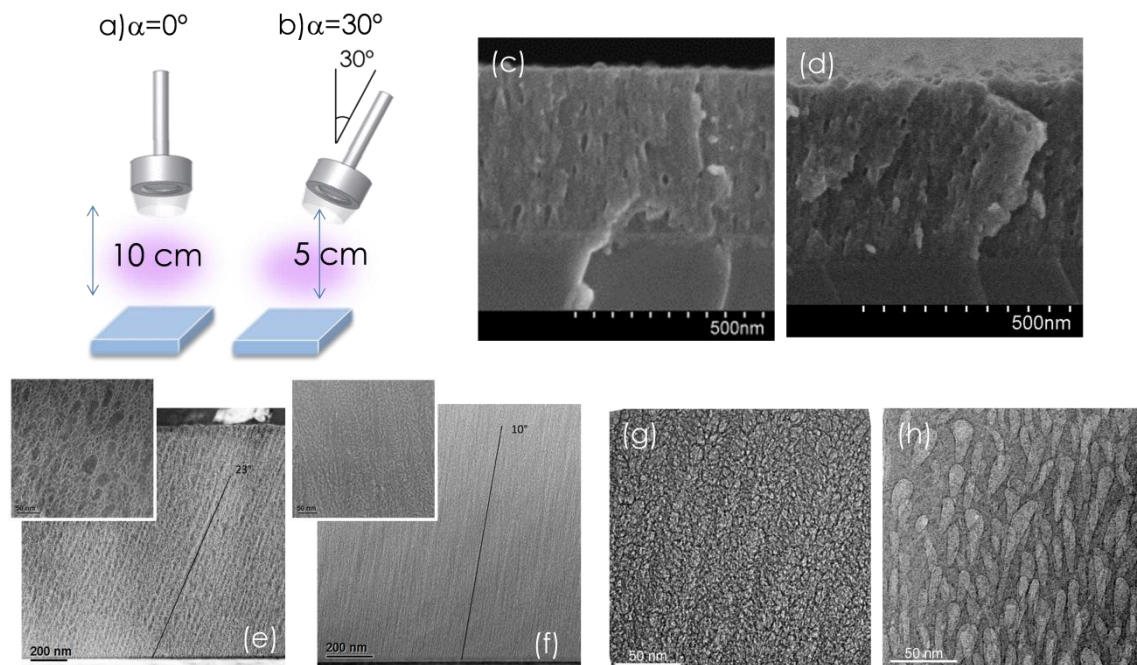


Figure 1 – Setups used for producing the coatings studied: (a) and (b); (c) deposition at $\alpha=0$ (setup (a)); (d) deposition at $\alpha=30^\circ$ (setup (b)); influence of pressure on pore orientation for $\alpha=30^\circ$: (e) 3.0×10^{-2} mbar and (f) 7.2×10^{-2} mbar. Influence of power supplied to the target on the pore size (deposition at $\alpha=30^\circ$ and Helium pressure of 5.0×10^{-2} mbar): (g) 50 W and (h) 300 W.

Session 2

Nanomaterials for sustainable energy and protection of the environment

New Approaches in Heterogeneous Photocatalysis for Improved Environmental Applications

G. Colón

^a *Instituto de Ciencia de Materiales, Centro Mixto CSIC-US
Americo Vesputio, 49, Seville, Spain*

*contact e-mail: gcolon@icmse.csic.es

Keywords: photocatalysis, band tailoring, visible active

Abstract

Since they were first described in the scientific literature, photoinduced processes have been studied with focusing on several industrially oriented applications. Despite differences in their character and proposed utilization, most of the photoinduced processes that have been successfully exploited have the same origin. Thus, a semiconductor can be excited by light energy higher than the band gap which results in inducing the formation of energy-rich electron-hole pairs. In using the term photocatalysis, it is commonly understood that we are referring to any chemical process catalyzed by a solid where the external energy source is an electromagnetic field with wave numbers in the UV-visible-infrared range.

Typical semiconductors such as TiO₂, ZnO, SrTiO₃, CeO₂, WO₃, etc. can all act as photoactive materials for redox/charge-transfer processes due to their electronic structures which are characterized by a filled valence band and an empty conduction band. Among these heterogeneous semiconductors, TiO₂ is the most widely used photocatalytic material because it fulfills all of the above requirements as well as exhibiting adequate conversion values.¹ However, in spite of its high conversion values, the calculated quantum yield for the reactions studied is still appreciably low (certainly well below 10%). This is due to the low rate of photon absorption with respect to the overall sunlight incoming photons.

Within this framework, the central of current research considers the extension of the solid light absorption spectrum to the visible region. This should facilitate the use of sunlight as an inexpensive, renewable energy source, for the excitation energy of the photocatalytic processes. TiO₂ is a UV-absorbing material with band gap energy in the 3.0-3.4 eV range, which is dependent on several physicochemical parameters such as primary particle size and shape and surface characteristics among others. If the band gap energy is decreased to about 2.5 eV or certain localized midgap states having adequate (excitation) energies are present, these would fulfill the two main requirements for generating valuable sunlight-driven photosystems.

New and/or more efficient visible-light photocatalysts are being sought with a view to meeting the requirements of future environmental and energy technologies driven by solar energy. As Kudo *et al* pointed out, suitable band engineering is needed in order to develop new photocatalysts for visible light.² The band tailoring of inorganic semiconductors can be undertaken using different approaches: (i) the creation of

discrete electronic levels between the valence and conduction bands (this is normally achieved by doping or codoping in the case of oxides); (ii) the creation of a new valence band through the synthesis of novel compounds; (iii) the formation of solid solutions exhibiting band gap values intermediate between those of the parent materials. Within this context, a research strategy has emerged in recent years that considers a new set of materials unrelated to TiO₂.

In summary, the complex combination of all these concepts into a composite system may be possible. If so it would drive the development of optimum systems which would maximize the photoactivity “*a la carte*” with tools allowing remote, dark activity, plasmonic and/or cooperative effects at interfaces and/or any other physicochemical method already mentioned as required by the specific application.

References

- [1] A. Kubacka, M. Fernández-García, G. Colón, *Chem. Rev.* **112** (2012) 1555.
- [2] A. Kudo, H. Kato, I. Tsuji, *Chem. Lett.* **33** (2004) 1534.

Investigation of the catalyzed hydrolysis of Ammonia Borane in a continuous flow reactor for the hydrogen production at medium scale

M. Paladini*¹, G.M. Arzac¹, D. Hufschmidt¹, G. Adame², M.A. Jiménez², A. Fernández¹

¹*Instituto de Ciencia de Materiales de Sevilla (ICMS), CSIC-Universidad de Sevilla. C/ Américo Vespucio 49. Isla de la Cartuja, 41092 Seville, Spain.*

²*Abengoa Hidrógeno, Campus Palmas Altas, Sevilla.*

[*mariana.paladini@icmse.csic.es](mailto:mariana.paladini@icmse.csic.es)

(+34 954 909 231)

Keywords: ammonia borane, cobalt boride, hydrolysis, hydrogen generation, continuous flow reactor.

Abstract

Ammonia Borane (NH₃BH₃, AB) currently is attracting a considerable attention because of its hydrogen storage capability (19.6% wt hydrogen content) [1]. AB produces hydrogen of high purity through hydrolysis according to (1), in a safe and easily controllable reaction.



This work presents a study of the hydrolysis of AB according to equation (1) in a continuous flow reactor employing a Co-B catalyst supported on a monolith made from stainless steel prepared in the laboratory [2,3]. The stability of AB fuel solution has been studied under different chemical conditions (buffer, NaOH etc.). In addition to the well know storage method under Ar [4] storage under N₂ atmosphere was investigated as well. The continuous hydrogen production in a scale of 0.5 L·min⁻¹ was tested. Several parameters of the reaction, the flow rate of the fuel solution, its concentration of AB and the mass of the supported catalyst, have been investigated with the aim to produce hydrogen at a constant temperature, flow rate and a maximum conversion.

Figure 1 shows the hydrogen generation rate (HGR) curve for a 10% wt AB fuel with an addition rate of 2-3 mL·min⁻¹ to produce hydrogen in the order of 0.35-0.4 L·min⁻¹ at a constant temperature about 70°C. After an initializing period of ca. 20 min a rather constant and stable Hydrogen generation can be observed. The durability of the catalyst has been assessed in cycles of 30 minutes.

The fresh and used catalyst has been characterized by means of SEM and XRD. No reaction products were found to have precipitated inside the reactor for short reaction times; however a precipitate was found in the residue tank. Analysis of this by XRD (figure 2) showed a mixture of NH₄B₅O₈·4H₂O and (NH₄)₂B₄O₇·4H₂O as products of the hydrolysis. The conversion of AB was measured in a volumetric way, determining the hydrogen produced from a sample taken from the fuel solution using an excess of catalyst. The conversion measured by the volumetric method was 91%.

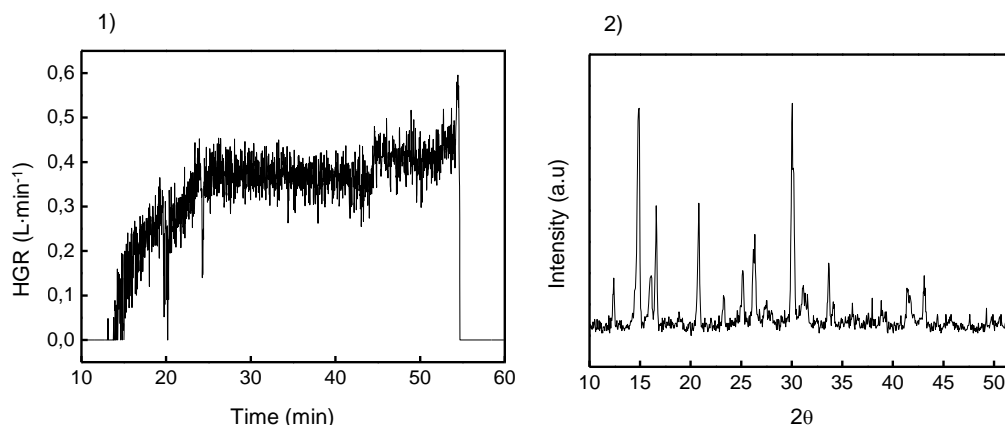


Figure 1 – Hydrogen generation rate (HGR) curve for the AB hydrolysis reaction in a continuous flow reactor.

Figure 2 – XRD pattern of the solid reaction product.

Acknowledgements: We kindly acknowledge the financial support from Abengoa Hidrógeno S.A., MINECO (Project CTQ2012-32519), “Junta de Andalucía” (TEP217) and the EC (CT-REGPOT-2011-1-285895, AL-NANOFUNC).

References

- [1] H.L. Jiang, Q. Xu, *Catalysis Today*, **170** (2011), 56-63.
- [2] G.M. Arzac, D. Hufschmidt, E. Jiménez Roca, A. Fernández Camacho, M.A. Jiménez Domínguez, S. Tyagi, M.M. Jiménez Vega, B. Sarmiento Marrón. *Proceso de producción de hidrógeno mediante hidrólisis catalítica en un reactor continuo para llevar a cabo dicho procedimiento*. Solicitante: Abengoa Hidrógeno S.A. Número de solicitud: P201230221 (14 de febrero de 2012).
- [3] G. M. Arzac, D. Hufschmidt, M.C. Jimenez De Haro, A. Fernandez, B. Sarmiento, M.A. Jimenez, M. M. Jimenez, *Int J Hydrogen Energy*, **37** (2012), 14373-14381.
- [4] M. Chandra et al, *J. Power Sources*, **159**, (2006) 855-860.

Chlorination of Toluene over Ionic Liquid grafted in Carbon Nanofiber

A. Martínez-Pascual^a, S. Ivanova^a, P. Losch^b, M. Boltz^b, B. Louis^b, F. Montilla^a J.A. Odriozola^a

Instituto Ciencia de Materiales de Sevilla

^a *Departamento de Química Inorgánica CSIC-Universidad de Sevilla
Sevilla, Spain*

^b *Laboratoire de Synthèse Réactivité Organique et Catalyse (LASYROC), UMR 7177,
Institut de Chimie, Université de Strasbourg, 1 rue Blaise Pascal, 67000
Strasbourg Cedex, France*

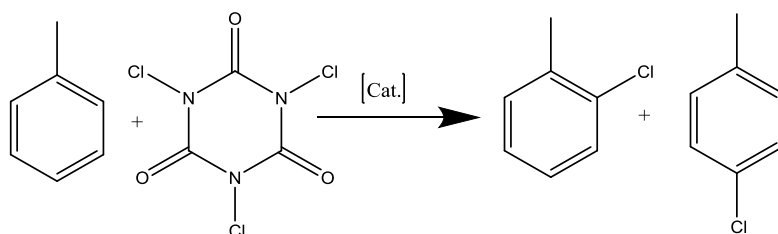
[*antonio.martinez@icmse.csic.es](mailto:antonio.martinez@icmse.csic.es)

Keywords: CNF, Ionic liquids, heterogenation of homogeneous catalysts, chlorination of toluene.

Abstract

The isomerically pure chloroaromatics are very valuable materials. They can serve as intermediates in the synthesis of compounds such as pesticides and pharmaceuticals. Unfortunately, the conventional methods for chlorination of aromatics in many cases result in a mixture of regioisomers, which are difficult to separate. During the past few years, considerable efforts have been devoted to the development of more efficient and selective aromatic chlorinations, including use of different reagent types, solvents, and catalysts [1].

The chlorination of the aromatic ring (as for example in toluene), is an electrophilic substitution process, which normally occurs at ortho and para positions. Both, ortho- and para-chlorotoluene, are used in the manufacture of a variety of products including pharmaceuticals, dyes, etc. p-chlorotoluene is more valuable than the o-chlorotoluene, and consequently much effort has been expended in the development of para-selective processes and catalyst/co-catalyst systems [2].



This reaction occurs at low temperature with CH_2Cl_2 , as a solvent and produces di- tri-substituted aromatics too.

Ionic liquids have attracted increasing interest as alternative to conventional organic solvents in the last years [3]. Ionic liquids represent a unique class of new reaction media for transition metal catalysis. Their non-volatile nature enables significant engineering advantages for distillative product separation and prevents uncontrolled evaporation. The possibility to specifically vary their physical and chemical properties make them ideal candidates for applications in biphasic catalysis [4]. Ionic liquids are using as co-catalyst and catalyst too.

In this work, we describe how immobilize, an ionic liquid, butyl methyl imidazolium (BMIM) over carbon nanofibres (CNF) were chosen for its low reactivity, by easily grafting ability and activation, avoiding the main drawback in homogeneous catalysis: the separation and recycling.

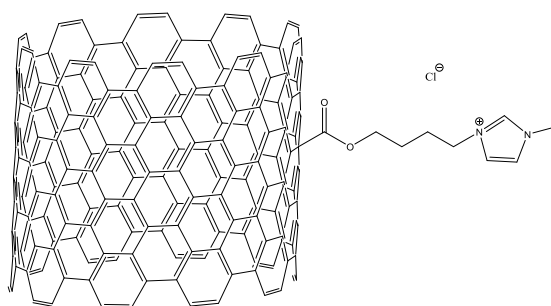


Figure 1. BMIM CNF supported

The synthesis was classified in 4 steps: Activation, Grafting, Functionalization and Catalyst build-in. It was followed by IR in 3 steps. In the first step, activation, CNF was mixed with nitric acid in a sonicated bath at 60°C during 24h. The second step, grafting, consist in the reaction between Activated-CNF and SOCl₂ in reflux to 70°C for 24h and it carried out under vacuum, in absence of water. The third step, functionalization, was to react with 3-Chloro-1-propanol, firstly, and 1-methyl-imidazole, after. The synthesis was conducted under vacuum, up to 77% yield. The fourth step, we added AlCl₃ in 11% and 22% in order to generate AlCl₄⁻ and Al₂Cl₇⁻ with the counterion Cl⁻ that stabilize to imidazolium. This BMIM CNF samples were characterized by TGA, TPO, SEM, Raman and IR.

The success of the BMIM grafting over nanofibers was 11%, calculated by TGA. This homogeneous catalysts is used for chlorination of toluene with TCCA reaction, giving a unexpected and promising results.

The reaction conditions at atmospheric pressure was 83°C and 500 rpm, for 96h and analyze by GC- analysis equipped with FID detector. The results was that this catalyzer have a great selectivity to *meta* position in chlorination on aromatic ring of toluene that is activated for electronic aromatic substitution with *orto* and *para* positions as preferential sites

	Conversion 96h	Conversion (%)	Selectivity Mono (%)	Selectivity Para (%)	Selectivity Ortho (%)	Selectivity Meta (%)
CNF-AL11%	5,41	100	46,05	36,49	17,45	
CNF-AL22%	7,2	100	37,56	34,18	28,26	

This fact may be explained by steric hindrance when the toluene, TCCA and Imidazole grafted to CNF interact and placing by a π Stacking interaction, and left *meta* position more available for chlorination.

References

1. A. Guy, M. Lemaire, J. P. Guette, *Tetrahedron* 1982, 38, 2339–2346.
2. Suzuki, T., and Komatsu, C., U.S. Patent 4,831,199 (1989), to Ihara Chemical Industry Co.
3. Min Jeong Park, Jae Kyun Lee, Bang Sook Lee, Yong-Won Lee, Insung S. Choi, and Sang-gi Lee, *Chemistry of Materials* 2006 18 (6), 1546-1551
4. P. Wasserscheid, W. Keim, *Angew. Chem. Int. Ed.* 2000, 39, 3772-3789

Plasmonics for beaming LED emission

G. Lozano^{a*}, S. R. K. Rodriguez^a, M. A. Verschuuren^b and J. Gomez Rivas^{a,c}

^a Center for Nanophotonics, FOM Institute AMOLF, High Tech Campus 4, 5656 AE, Eindhoven, Netherlands

^b Philips Research, High Tech Campus 4, 5656 AE, Eindhoven, Netherlands

^c COBRA Research Institute, Eindhoven University of Technology, 5600MB, Eindhoven, Netherlands

*contact e-mail: lozano@amolf.nl

Keywords: diffraction; fluorescence; LED; nanophotonics; plasmonics

Abstract

The development of efficient light sources based on light-emitting diodes (LEDs) is a central goal for solid-state lighting (SSL). The most widely employed route to achieve white light using LEDs consist in combining an electrically driven blue LED and a material, usually known as a *phosphor* that absorbs part of the blue light and emits in the green-to-red region of the electromagnetic spectrum.[1] The critical role played by this emitting material in SSL has guided most of material research efforts in this field. With the advent of stable and ultra-high efficient emitters, research in SSL is shifting towards more advanced ways of light generation and manipulation.

Metallic nanoparticles provide unique ways of controlling light at length scales smaller than the wavelength through the excitation of surface plasmons. During the last years, the field of surface plasmon polariton optics or plasmonics has moved from a domain in which fundamental insights were developed into a discipline that becomes relevant to applications.[2] However, there are not yet applications of plasmonic structures compatible with state-of-the-art SSL technologies.

Herein, we demonstrate that the emission of a phosphor-converted LED can be boosted by aluminum nanoparticles that enhance the directionality of the emitted light such that it is preferably emitted straight from the surface, rather than toward the side. The emission in this direction is enhanced by more than a factor of 60 for a specific color (see Fig. 1).[3] This directional enhancement is the result of the plasmonic enhanced excitation of the phosphor and its decay into collective plasmonic resonances supported by the array of nanoparticles.[4] These resonances, known as surface lattice resonances (SLRs), arise from the coupling of localized surface plasmon polaritons to diffracted orders in the array.[5,6] SLRs have a large spatial extension and can couple very efficiently to free space radiation due to their hybrid photonic-plasmonic character.[7] These features lead to a highly directional emission in defined directions which can be controlled by the shape and dimensions of the particles and by the lattice geometry.[8] This demonstration opens a new path for fundamental and

applied research in SSL in which plasmonic nanostructures are able to mold the emission with unprecedented precision.[3]

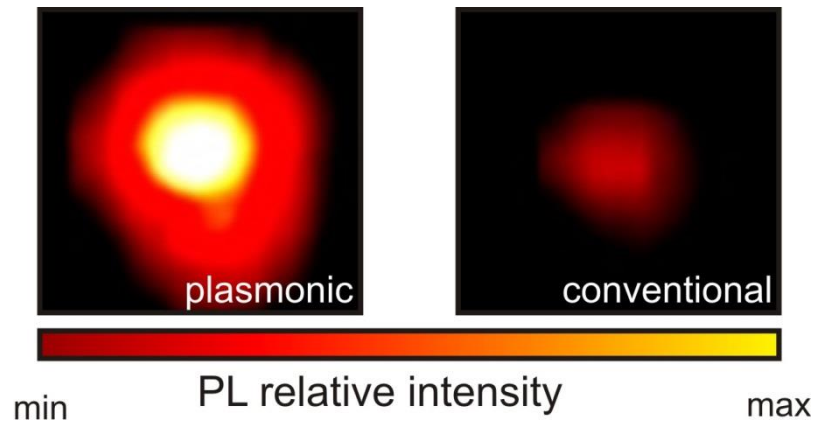


Figure 1 – . Digital camera pictures of the emission from a plasmonic LED (left) and a conventional phosphor-converted LED (right).

References

- [1] S. Pimputkar, S. J. DenBaars, S. Nakamura, *Nat. Photon.* **3** (2009) 180.
- [2] A. Polman, *Science* **332** (2008)868.
- [3] G. Lozano, D. J. Louwers, S. R. K. Rodríguez et al., *Light: Science & Appl.* **2** (2013) e66.
- [4] X. M. Bendaña, G. Lozano, G. Pirruccio, J. Gomez Rivas and F. J. Garcia de Abajo, *Optics Express* **21** (2013) 5636
- [5] G. Vecchi, V. Giannini, J. Gómez Rivas, *Phys. Rev. Lett.* **102** (2009) 146807.
- [6] V. Giannini, G. Vecchi, J. Gómez Rivas, *Phys. Rev. Lett.* **105** (2010) 266801.
- [7] S. Murai, M. A. Verschuuren, G. Lozano, G. Pirruccio, S. R. K. Rodriguez and J. Gomez Rivas, *Optics Express* **21** (2013) 4250
- [8] S. R. K. Rodríguez, G. Lozano, M. A. Verschuuren et al. *Appl. Phys. Lett.* **100** (2012) 111103.

Resonant Photocurrent Generation in Dye-Sensitized Periodically Nanostructured Photoconductors by Optical Field Confinement Effects

M. Anaya^{a*}, M. Calvo^a, J.M. Luque^a, H. Míguez^a

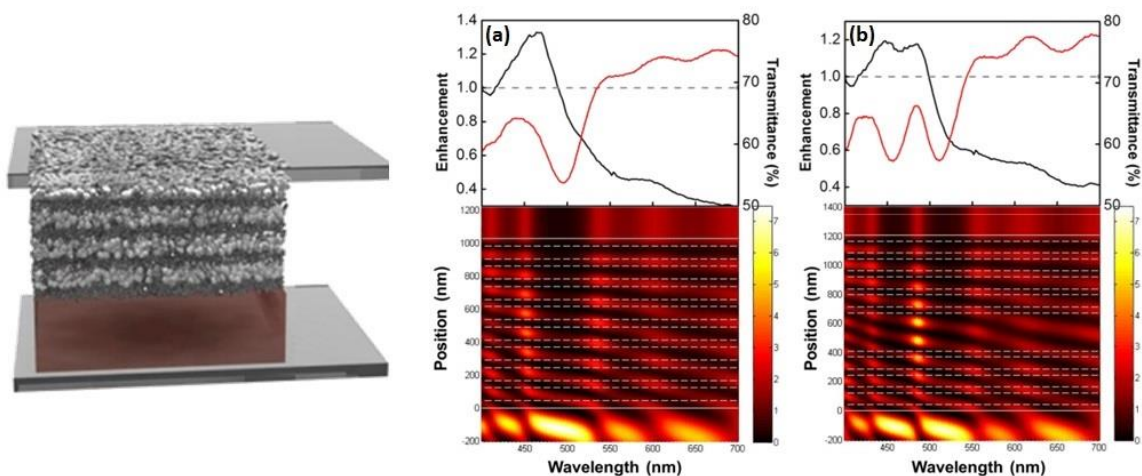
^aInstituto de Ciencia de Materiales de Sevilla, Américo Vespucio 49, Sevilla, 41092, ES

*contact e-mail: Miguel.anaya@csic.es

Keywords: photocurrent, optical absorption, resonant enhancement.

Abstract

Herein we show experimental evidence of resonant photocurrent generation in dye sensitized periodically nanostructured photoconductors. These materials were attained by the alternating deposition of layers of TiO₂ nanoparticles with different porosity to produce a spatial modulation of the refractive index in one dimension of the space.^[1] We have built both periodic and broken symmetry nanostructured photoconducting TiO₂ multilayers with enough number of periods as to display different types of photon resonances that confine the field within the material in different ways. The resonant photocurrent finds their foundations in light confinement effects that were achieved by spectral matching of the sensitizer absorption band to different types of localized photon modes present in either periodical or broken symmetry structures. Results are explained in terms of the calculated spatial distribution of the electric field intensity within the configurations under analysis.^[2] Such simulations were performed using a code written in MatLab and based on the transfer matrix method. A direct relation between resonant photon modes and photon-to-electron conversion peaks can be established. We foresee this sort of structures could allow the development of photo-electro-chemical devices with finer spectral control over light absorption.



Left: System design. **Right:** Spectral variation of the photocurrent enhancement factors for (a) periodic arrangement of layers and (b) a resonator built by depositing a thicker middle layer

within a periodic multilayer (black solid lines). The respective transmittance spectra are also plotted (red solid lines). In the bottom panels, the calculated spatial distribution of the electric field along a cross section of both types of structures is plotted as a function of the incident wavelength.

References

- [1] Calvo, M.E.; Colodrero, S.; Rojas, T.C.; Anta, J.A.; Ocaña, M.; Míguez, H.; *Adv. Func. Mater.*, 18 (2008), 2708-2715.
- [2] Anaya, M.; Calvo, M.E.; Luque, J.M.; Míguez, H., *J. Am. Chem. Soc.*, DOI: 10.1021/ja401096k.

Periodical structures to improve light harvesting in Dye Solar Cell

Carmen López-López*, Silvia Colodrero and Hernán Míguez.

Instituto de Ciencia de Materiales de Sevilla, Consejo Superior de Investigaciones Científicas-Universidad de Sevilla, Américo Vespucio 49, 41092, Sevilla, Spain.
carmen@icmse.csic.es

Keywords: Dye Solar Cell, Photonic Crystal, Diffraction grating.

Abstract

Dye solar cells (DSCs) are photovoltaic devices in which the absorption of sunlight is realized by dye molecules attached to the surface of a titanium dioxide (TiO_2) electrode. Many strategies followed to enhance the efficiency of these cells are based on increasing the residence time of photons in the active electrode. This is commonly achieved by including diffuse scattering layers coupled to the photoanode, which implies that the cell becomes opaque, losing its semitransparency and hence one of its more interesting added values for building integrated photovoltaics (BIPV). Herein we show alternative approaches to the optical design of DSCs based on two different periodic structures, which improve light harvesting in the cell while preserving part of its transparency in the visible region of the spectrum.

The first one consists on coupling nanoparticle based one dimensional photonic crystals (1DPCs)¹⁻⁵ to the TiO_2 electrode. These coherent mirrors present a high reflectance in a targeted wavelength range in which the dye absorption enhancement is observed. Alternatively, we also propose the use of a diffraction grating. In this case, the TiO_2 electrode is molding by soft lithography to obtain the periodical structure. In these cells the current enhancement is obtained because light is diffracted back to the dyed layer.

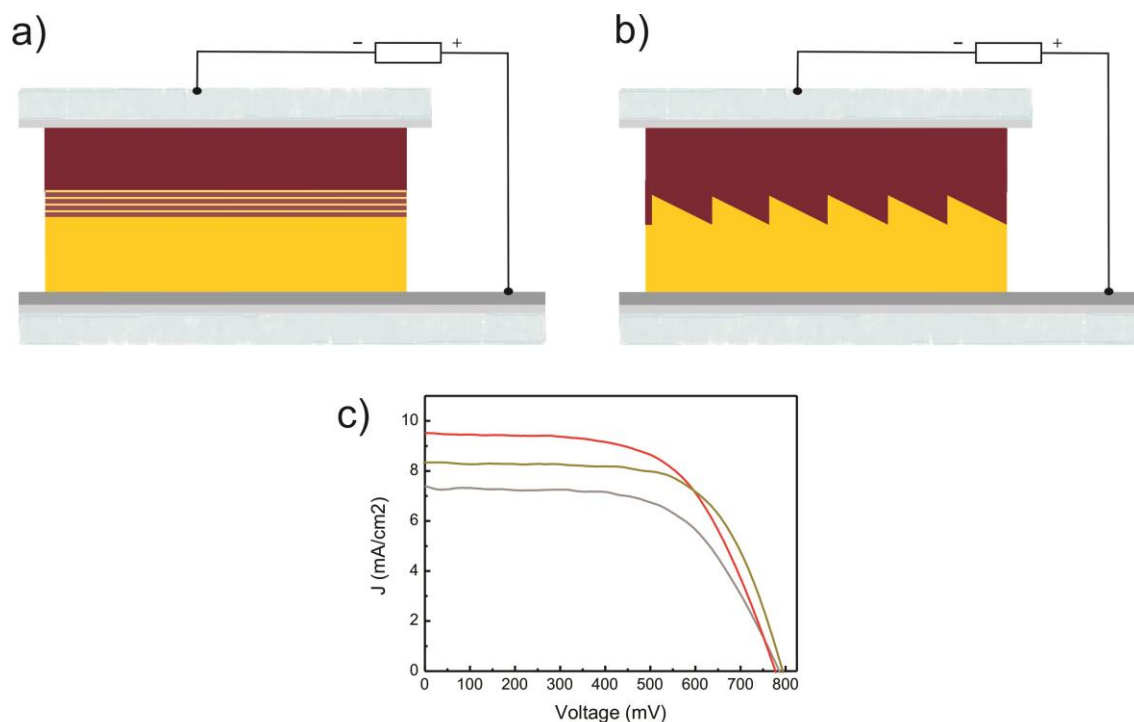


Figure 1 – Schemes of DSCs in which a) a 1DPC and b) a diffraction grating has been integrated. c) IV curves measured for a reference cell (grey line), a 1DPC based cell (red line) and a diffraction grating based cell (dark yellow line).

References

- [1] Colodrero, S.; Mihi, A.; Häggman, L.; Ocaña, M.; Boschloo, G.; Hagfeldt, A.; Míguez, H.; Porous One-Dimensional Photonic Crystals Improve the Power-Conversion Efficiency of Dye-Sensitized Solar Cells, *Adv. Mater.*, **2009**, 21, 764-770.
- [2] López-López, C.; Colodrero, S.; Raga, S.R.; Lindström, H.; Fabregat-Santiago, F.; Bisquert, J.; Míguez, H.; Enhanced diffusion through porous nanoparticle optical multilayers, *J. Mater. Chem.*, **2012**, 22, 1751-1757.
- [3] Colodrero, S.; Forneli, A.; López-López, C.; Pelleja, L.; Míguez, H.; Palomares, E.; Efficient Transparent Thin Dye Solar Cells Based on Highly Porous 1D Photonic Crystals, *Adv. Funct. Mater.*, **2012**, 22, 1303-1310.
- [4] Colonna, D.; Colodrero, S.; Lindström, H.; di Carlo, A.; Míguez, H.; Introducing structural colour in DSCs by using photonic crystals: interplay between conversion efficiency and optical properties *Energy & Environmental Science*, **2012**, 5, 8238-8243.
- [5] López-López, C.; Colodrero, S.; Calvo, M.E.; Míguez, H.; Angular response of photonic crystal dye sensitized solar cell, **2013**, 6, 1260-1266.

Tailored luminescent emission of dyes embedded in porous resonators

A. Jiménez-Solano^{a*}, J. M. Luque^a, M. E. Calvo^a, ; F. Fernández-Lázaro^b, ; H. Míguez^a.

^a Consejo Superior
de Investigaciones Científicas (Spain)
^b Univ. Miguel Hernández de Elche (Spain)

*contact e-mail: alberto.jimenez@icmse.csic.es

Keywords: luminescent, one-dimensional photonic crystals, colloidal crystal

Abstract

Here we study the light emitted from different hybrid organic dye doped inorganic nanoparticle-based one dimensional (1D) photonic crystal (PC) architectures. The increase in the photon density of states caused by confinement in very specific slabs of the multilayer implies a lower photon group velocity,^[1] which in turn yields longer light-matter interactions. We investigate both experimentally and theoretically^[2] how the angular distribution of light emitted from these 1DPC structures is modified depending on the spectral matching of either resonant or stop band modes of the PC. Our measurements are explained in terms of the electromagnetic field distribution in the photonic structure. These results prove that by changing the photonic environment of a dye, it is possible to finely tune its optical response throughout the visible.

References

- [1] Bendickson, J. M.; Dowling, J. P.; Scalora, M. *Phys. Rev. E*, **53** (1996), 4107.
[2] Lozano, G.; Colodrero, S.; Caulier, O.; Calvo, M.E.; Míguez, H. *J. Phys. Chem. C*, **114** (2010), 3681.

Optofluidic Sensors Based on Nanoporous Bragg Microcavities prepared by GLAD

M. Oliva-Ramirez^{a*}, L. González-García^a, J. Parra-Barranco^a, F. Yubero^a, A. Barranco^a and A. R. González-Elipe^a.

^a *Instituto de Ciencia de Materiales de Sevilla, CSIC-Uni, Sevilla, Sevilla, Spain*
*contact e-mail: manuel.oliva@icmse.csic.es

Keywords: Bragg microcavities, Porous layers, Optofluidics, GLAD thin films, liquids analysis, responsive optical systems.

Abstract

Porous Bragg microcavities formed by stacking porous nanocolumnar layers of different refraction index materials (SiO_2 and TiO_2) have been prepared by physical vapor deposition at glancing angles (GLAD). Figure 1(a) shows a SEM micrograph and 1 (b) a sketch of the utilized multilayer structure. Microcavities with different optical properties can be obtained by changing the thickness and the evaporation angle of the TiO_2 and SiO_2 layers. The microcavity structures have been implemented into responsive devices to characterize liquids, mixtures of liquids or solutions flowing through them (figure 1 (c)). The large displacements observed in the optical spectral features (Bragg reflector gap and resonant peak) of the photonic structures have been quantitatively correlated with the refraction index of the circulating liquids (figure 1(d)). Experiments carried out with different glucose and NaCl solutions and mixtures water plus glicerol illustrate the potentialities of these optofluidic devices to determine the concentration of the solutions or the proportion of two compounds in a liquid mixture.

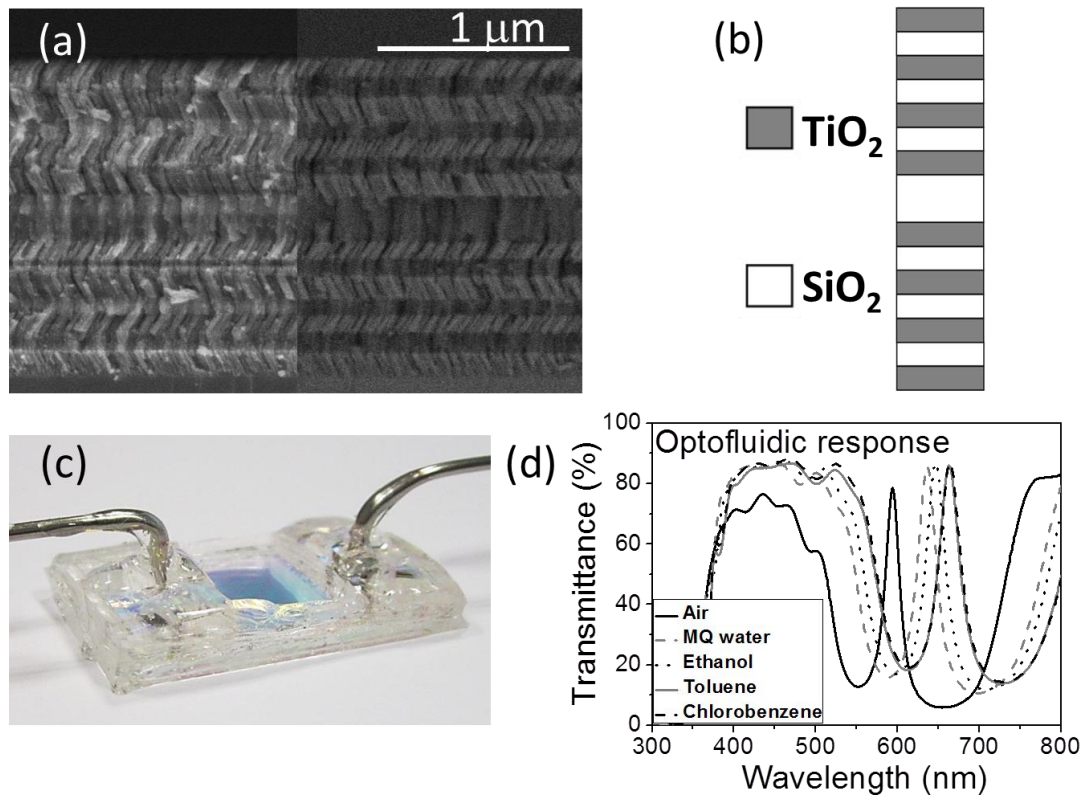


Figure 1 – (a) and (b) SEM and sketch of the multilayer; (c) experimental microfluidic device; (d) optofluidic response with different liquids.

Posters

BiPO₄ nanostars for luminescent applications

Criado Joaquín, Becerro Ana I.*, Gontard L.C., Fernández A. and Ocaña M.

*Instituto de Ciencia de Materiales de Sevilla(CSIC-University of Sevilla) c/ Américo
Vespucio, 49. 41092 Sevilla (Spain)*

*contact e-mail: anieto@icmse.csic.es

Abstract

There has been recently an increase research on nanostructured rare earth (RE) compounds owing to their critical importance in the fields of integrated optical systems and biomedical applications, among others [1-5]. Lanthanide orthophosphates (LnPO₄) represent an important class of materials because they possess a variety of favorable thermal, chemical and optical properties. However, it is always desirable to have a non-lanthanide based phosphate host with all the LnPO₄ properties. This is because high purity lanthanide ions are essential when LnPO₄ are used as host materials for luminescent applications, and obtaining large quantities of lanthanides in a highly pure form is extremely difficult and much more costly compared to main group elements. Motivated by this circumstances, BiPO₄ has been widely used as a model host for Eu³⁺ as a dopant for the following reasons: *i)* BiPO₄ is isostructural to LnPO₄,[6] *ii)* the dopant Eu³⁺ and the framework Bi³⁺ have the same oxidation state and similar ionic radii [7] and, therefore, substitution of Bi³⁺ by Eu³⁺ is, in principle, plausible.

The physicochemical properties of nanomaterials are strongly associated with their size and morphology, and this applies especially to the optical properties of luminescent materials. However, in spite of the numerous studies about BiPO₄, little attention has been paid to the fabrication of homogeneous, monodisperse BiPO₄ nanoparticles that can act as nanophosphors after doping with appropriate active lanthanide ions.

Herein, we report the synthesis of monodisperse, monoclinic BiPO₄ particles with a new, unusual morphology consisting of several nanorods (150 nm x 30 nm) arranged in a star-like hierarchical structure (Figure 1). They were synthesized in an air-force oven at 120°C for 20 hours using H₃PO₄, Bismuth nitrate and a glycerol/ethylenglycol (Gli/EG) mixture as solvent and sodium citrate as capping agent. Changing any of the experimental conditions (Gli/EG ratio, temperature, time and Bi, P or citrate concentrations) led to either a gel-like structure or to micrometric cocoon-like structures. The morphology was maintained after doping with up to 2.5% Eu³⁺. Higher Eu contents did not allow keeping the star-like shape. The luminescent properties of the Eu-doped BiPO₄ nano-stars phosphors were subsequently analyzed and discussed.

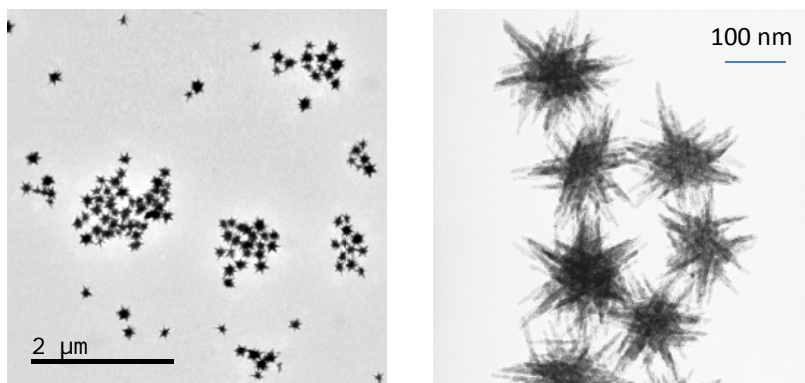


Figure 1 – TEM micrographs of BiPO₄ nanoparticles at different magnifications.

References

- [1] Zhong, SL; Lu, Y; Gao, MR; Liu, SJ; Peng, J; Zhang, LC; Yu, SH. *Chem. A Eur. J.* **18** (2012) 5222.
- [2] Pedersen H. and Ojamae L. *Nano Lett.* **6** (2006) 2044.
- [3] Mu Q.Y.; Wang Y.D. *J. Alloys Comp.* **509** (2011) 2060.
- [4] Ocaña M., Cantelar E. and Cussó F. *Mater. Chem. Phys.* **125** (2011) 224.
- [5] Rodríguez-Liviano, S; Aparicio, FJ; Rojas, TC; Hungria, AB; Chinchilla, LE; Ocaña, M. *Cryst. Growth Design* **12** (2012) 635.
- [6] Romero B.; Bruque S.; Aranda M.A.G.; Iglesias J.E. *Inorg. Chem.* **33** (1994) 1869.
- [7] Shannon R.D. *Acta Cryst.* **A32** (1976) 751.

Photocatalytic degradation of phenol over TiO₂. Effect of the TiO₂ surface treatment by fluorination or sulfation

J.J. Murcia Mesa^{a*}, M.C. Hidalgo López^a and J.A. Navío Santos^a

^a Instituto de Ciencia de Materiales de Sevilla (ICMS), Consejo Superior de Investigaciones Científicas CSIC - Universidad de Sevilla, Américo Vespucio 49, 41092 Sevilla, Spain

*contact e-mail: julie.murcia@icmse.csic.es, jjuliejoseane@hotmail.com

Keywords: Phenol, photocatalysis, S-TiO₂, F-TiO₂

Abstract

TiO₂ heterogeneous photocatalysis is a promising method for the destruction of contaminants, such as phenol, in water sources by using solar or artificial light illumination. TiO₂ properties; such as phase composition and structures, surface hydroxyl groups, particle size and surface defects play a very important role in the activity of this oxide in photocatalytic reactions. In different studies, some of these parameters have been modified in order to enhance the photocatalytic performance of the TiO₂ [1,2].

It has been reported that sulfation pre-treatment leads to stabilize TiO₂ surface area against sintering and anatase crystalline phase during the calcination process. A dehydroxylation process of the excess of adsorbed protons takes place during calcination, leading to the creation of surface oxygen vacancies, promoting the separation of photogenerated charges, thus improving the TiO₂ photocatalytic efficiency [1]. Fluorinated TiO₂ surface favors the generation of free OH radicals, which improves the photo-oxidation process [2].

In this work the influence of the TiO₂ surface modification by sulfation and fluorination of this oxide and relations between TiO₂ surface properties and activity results have been studied. Three different TiO₂ powders were evaluated in phenol photodegradation: Firstly TiO₂ was prepared by sol-gel method (TiO₂ SG), and then it was modified by impregnation with a H₂SO₄ 1 M solution (S-TiO₂). A third powder (F-TiO₂) was obtained by impregnation of the TiO₂ SG with a NaF 0.01 M solution. After impregnation (1h), filtration and drying, the powders were calcined at 650 °C for 2 h.

A summary of characterization results is shown in Table 1. As it can be seen TiO₂ SG presents the lowest specific surface area (S_{BET}) and the lowest anatase crystallite size (D), as a consequence of the transformation of anatase to rutile phase during the calcination process. The band gap value of TiO₂ SG decreases slightly after sulfation or fluorination treatment (Table 1).

Anatase is the only crystalline phase present in S-TiO₂ and F-TiO₂ samples while rutile can also be detected in unmodified TiO₂ (Fig. 1-A). In Fig. 1-B, a slight shift of the absorption to the visible region was observed for F-TiO₂ catalyst.

Photocatalytic activity tests show that phenol photodegradation rates (PDR) can be significantly enhanced by TiO₂ surface fluorination.

Table 1. Summary results.

	S _{BET} (m ² /g)	D _{ANATASE} (nm)	Band gap (eV)	PDR (mg Phenol. L ⁻¹ .s ⁻¹)
TiO ₂ SG	46	17	3.30	2.72x10 ⁻³
S-TiO ₂	58	20	3.20	4.76 x10 ⁻³
F-TiO ₂	51	24	3.18	1.00 x10 ⁻²

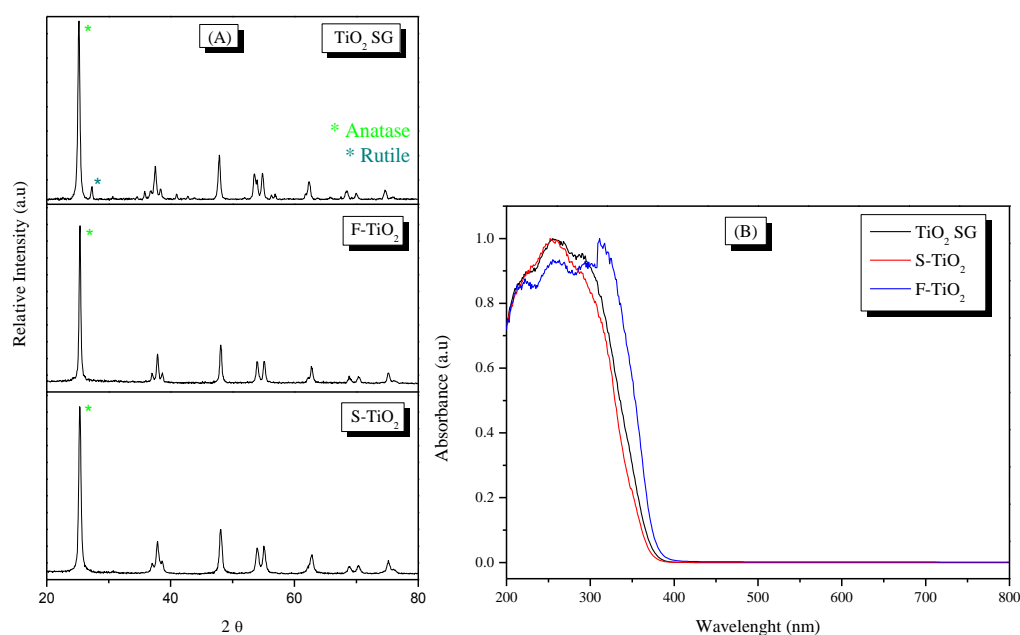


Figure 1 – (A) XRD patterns and (B) UV-Vis DRS spectra for TiO₂ powders.

References

- [1] M.C. Hidalgo, M. Maicu, J.A. Navío, G. Colón, *Appl. Catal., B*, **81** (2008) 49-55.
- [2] C. Minero, G. Mariella, V. Maurino, E. Pelizzetti, *Langmuir*, **16** (2000) 2632-2641.

An electron microscopy study of the nanostructure of collagen fibrils

S. Borrego-González^a, J. Becerra^{b,c}, A. Díaz-Cuenca^{a,c*}

^a *Instituto de Ciencia de Materiales de Sevilla (ICMS), Centro Mixto CSIC-Universidad de Sevilla, Avda. Américo Vespucio 49, Isla de la Cartuja, 41092 Sevilla, Spain*

^b *Departamento de Biología Celular, Genética y Fisiología Celular, Facultad de Ciencias, Campus de Teatinos, Universidad de Málaga, 29071 Málaga, Spain*

^c *Networking Research Center on Bioengineering, Biomaterials and Nanomedicine (CIBER-BBN), Spain*

*sara.borrego@icmse.csic.es ; aranzazu@icmse.csic.es

Keywords: collagen fibril, FE-SEM, STEM, D-periodicity

Abstract

The development of scaffolds mimicking the native bone tissue structure is a challenge in bone tissue engineering. The structure of bone is arranged in hierarchical levels from the individual constituents of hydroxyapatite and collagen fibrils, to the nanostructure of an interpenetrating mineralized collagen network, the lamellar microstructure of osteons and the final macrostructure of cancellous and cortical bone [1]. Type I collagen forms more than 90% of the organic mass of bone and provides the innate biological information required for cell adhesion, proliferation and orientation, and promotes the chemotactic response [2]. Therefore, collagen-based scaffolds must hold the structure of the natural collagen fibril, with characteristic D-periodicity of 67 nm and diameters around 100 nm, formed by the assembly of soluble collagen basic building blocks molecules [3]. Through a fibril, the triple-helical molecules are all parallel, but their ends are separated by gap zones of about 35 nm and overlap zones of 32 nm. Furthermore, the neighboring triple-helical molecules are offset or staggered by 67 nm [3,4].

This study focuses on the structural characterization at nanoscale level of a native bovine skin collagen sponge scaffold by FE-SEM and STEM using a Hitachi S-4800 Field Emission SEM. We have investigated different aspects in the sample preparation including the grid support and the sample holder, the fixation, the staining and the final coating treatments in order to optimize collagen nanostructure observations. This work will provide us with a very interesting tool to analyse collagen structural features in our research of the development of new collagen based porous scaffolds for bone tissue engineering applications.

Figure 1 displays a STEM image of a typical collagen micro fibril showing the 67 nm D-period.

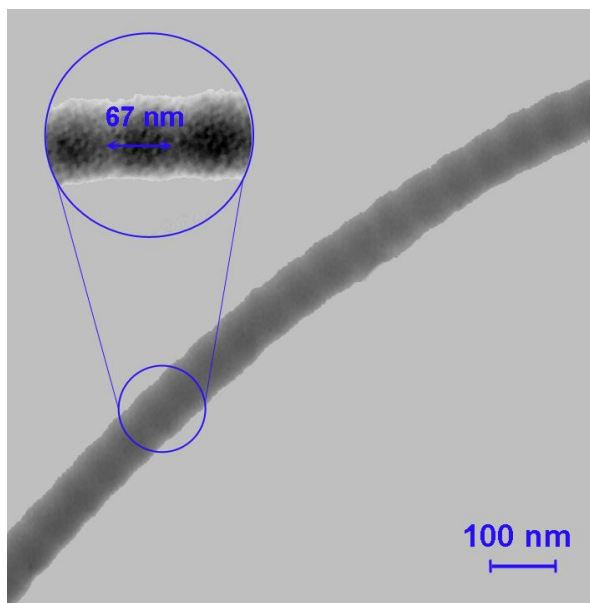


Figure 1 – STEM image showing a collagen fibril D-spacing (D-period)

Acknowledgements

We gratefully acknowledge the financial support provided by the Spanish Ministry of Science and Innovation (BIO2009-13903-C02-02), the Andalusian Ministry of Economy, Science and Innovation (Proyecto Excelencia CTS-6681), S. B-G is a fellow from the Andalusian Government Predoctoral Programme. We thank Dr. M.C. Jiménez de Haro for her assistance with the microscopy observations.

References

- [1] S. Weiner, H. D. Wagner, *Annual Review of Materials Science*, **28** (1998), 271–298.
- [2] A.M. Ferreira, P. Gentile, V. Chiono, G. Ciardelli, *Acta Biomaterialia*, **8** (2012), 3191-3200.
- [3] P. Fratzl, R. Weikamer, *Progress in Materials Science*, **52** (2007), 1263-1334.
- [4] K. Gelse, E. Pöschl, T. Aigner, *Advanced Drug Delivery Reviews*, **55** (2003), 1531-1546.

Fabrication and characterization of “small-molecules” core@shell nanowires

A. Nicolas Filippin, Maria Alcaire, Angel Barranco and Ana Borrás*

*Nanotechnology on Surfaces Lab., Materials Science Institute of Seville (ICMS), CSIC-
University of Seville, C/ Américo Vespucio 49, 41092, Seville (Spain)*

*contact e-mail: anaisabel.borras@icmse.csic.es; alejandro.filippin@icmse.csic.es

Keywords: nanowire, heterostructure, phthalocyanine, plasma polymerization, ESEM

Abstract

The fabrication of organic nanowires and nanofibers has gained attention due to their potential applications in fields photonic devices, organic field effect transistors (OFETs), phototransistors and solar cells [1]. Besides, the crystalline organic 1D nanostructures based on pi-conjugated molecules are presented as ideal candidates for fundamental studies, being the organic nanowires a model system in the study of transport mechanisms and properties-structure relationships. On other hand, a continuous evolution of the repertoire of available materials processing and device fabrication technologies has in turn driven the exploration of increasingly more-complex nanostructures. Very recently we have reported a universal method for the growth of single crystal organic nanowires (ONWs) formed by “small-molecules” on metal and non-metal substrates. This protocol is based on physical vapor deposition (PVD) of the organic molecules on substrates at controlled temperatures. In our previous works we have combined this method with other vacuum related procedures in order to fabricate different hybrid and heterostructured 1D nanostructures. For instance, the formation of metal decorated organic nanowires by deposition of metal nanoparticles by sputtering dc or controlled plasma etching of metal-organic nanowires [2]. And, very recently, the fabrication of organic/inorganic core/shell nanowires by plasma enhanced chemical vapor deposition of different semiconducting oxides on the as-grown organic nanowires [Fig. 1]. Herein we present a step forward in the controlled formation of heterostructured nanowires. Concretely, we explore the formation of amorphous-organic/crystal-organic core/shell nanowires by combination of the single crystal ONWs growth by PVD and the remote plasma deposition of “small-molecules” within the phthalocyanine family. The main aspects of the methodology are introduced paying special attention to the control on the plasma activation of the metal-organic molecules (metal-phthalocyanines and metal-porphyrins) with no damage of the single-crystal structure of the organic core and avoiding the formation of metal clusters in the amorphous-organic to crystal-organic interface. The characterization of the nanowires by SEM, STEM, SAED and HRTEM is presented and their optical properties analyzed.

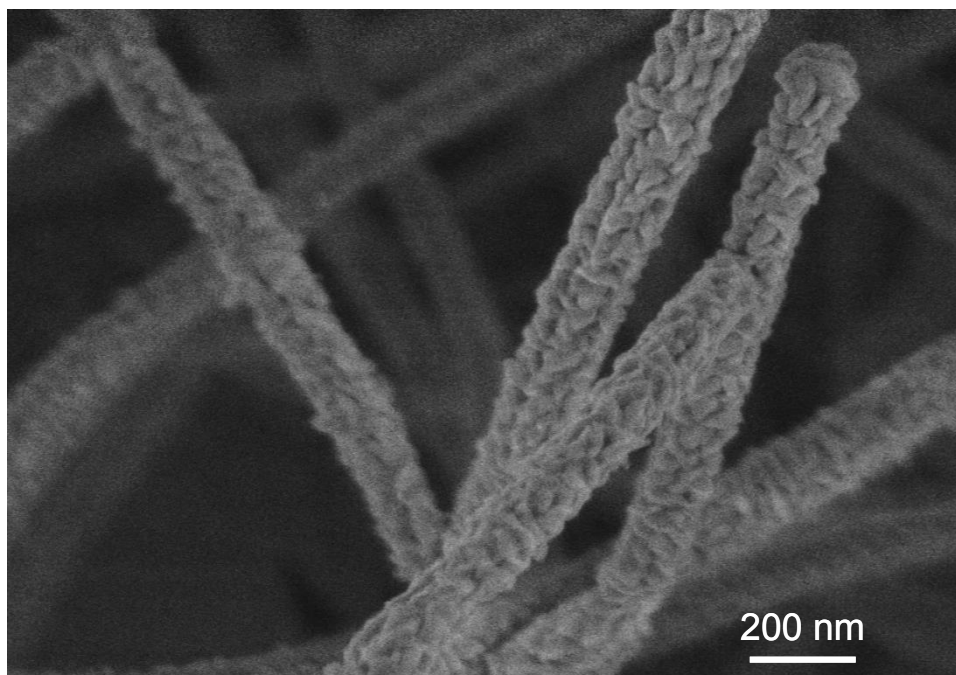


Figure 1. Conformal plasma growth of CuF₁₆Pc onto CoPc.

References

- [1] Briseno A.L., Mannsfeld S. C. B., Jenekhe, S. A., Bao Z., Xia, Y.; *Mater. Today*; **11** (2008), 38-47.
- [2] A. Borrás, O. Gröning, J. Köble, P. Gröning; *Advanced Materials*; **21** (2009), 4816-4819.
- Alcaire M., Sanchez-Valencia J.R., Aparicio F.J., Saghi Z., Gonzalez-Gonzalez J.C., Barranco A., Zian Y.O., Gonzalez-Elipe A.R., Midgley P., Espinos J.P., Gröning P., Borrás A.; *Nanoscale*; **3** (2011), 4554-4559.
- [3] M. Macias-Montero, A. N. Filippin, Z. Saghi, F. J. Aparicio, A. Barranco, J. P. Espinos, F. Frutos, A. R. Gonzalez-Elipe and A. Borrás *Advanced Functional Materials* DOI: 10.1002/adfm.201203390.

Mean inner potential and skeletal density of zeolite MCM- 41 using TEM

Lionel C. Gontard^{a*}, Rafal E. Dunin-Borkowski^b, T. Kasama^c

^a Instituto de Ciencia de Materiales de Sevilla (CSIC), 41092, Sevilla, Spain

^b Ernst Ruska-Centre for Microscopy and Spectroscopy with Electrons and Peter Grünberg Institute, Forschungszentrum Jülich, D-52425 Jülich, Germany

^c Center for Electron Nanoscopy, Technical University of Denmark, DK-2800 Kgs. Lyngby, Denmark

*contact e-mail: lionel.cervera@icms.csic.es

Keywords: MCM-41, zeolite, TEM, tomography, holography

Abstract

Zeolites are aluminosilicates widely applied as support for catalysts in the chemical industry. We have used electron holography tomography (EHT) to characterise in three-dimensions inside and outside two MCM-41 zeolite nanoparticles (Figure 1A) the electrostatic potential and the charge density [1]. Moreover, we estimate the skeletal density of the zeolites from the three-dimensional electrostatic potential (Figure 1B). The composition of the sample, measured using energy-dispersive x-ray spectroscopy (EDX-TEM), is very close to silicon dioxide (SiO₂). Figure 1C is a high-magnification TEM image showing that the zeolite examined here is formed by an hexagonal ordered structure of amorphous SiO₂ and empty channels with a diameter of 1 nm. Insets in Figure 1C show a model and a magnified image of an unit cell of the channelled structure. Because SiO₂ is not a good electrical conductor during transmission electron microscopy observation the sample accumulated an electric charge. This effect implies that the electrostatic potential (shown in Figure 1B) has in first approximation two terms

$$V(x, y, z) = V_o(x, y, z) - |V_c(x, y, z)|$$

the first term $V_o(x, y, z)$ is called the mean inner potential (MIP), an average electrostatic potential that depends on the structure and composition of the unit cell of the sample. The second term $|V_c|$ accounts for the contribution of the induced charge due to secondary emission during TEM observation (in typical TEM experiments its effect is to decrease the mean inner potential [2]). The density of electric charge induced in the sample is not homogeneous: It is small inside the particles (small $|V_c|$) and large close to the surfaces of the sample (large $|V_c|$) [2]. Correspondingly, the potential measured experimentally in Figure 1B reaches a maximum value of 14 Volts inside the particles and decreases towards their surfaces. The spatial resolution of EHT does not resolve the channelled structure of the zeolite, and the potential must be divided by 2 to get the real potential. Then, the potential inside the particle where the contribution of charging is minimum (therefore close to the real value of the MIP) is approximately 7 volts.

The curve in Figure 1D shows MIP values of MCM-41 for a realistic range of density values of SiO₂, calculated using a binding-approximation [4], and the unit cell sketched

in the inset of Figure 1C. Comparing the curve with the experimental value of $MIP \cong 7$ V we estimated the skeletal density of the MCM-41 zeolite nanoparticles to be approximately 2.1 gr/cm^3 .

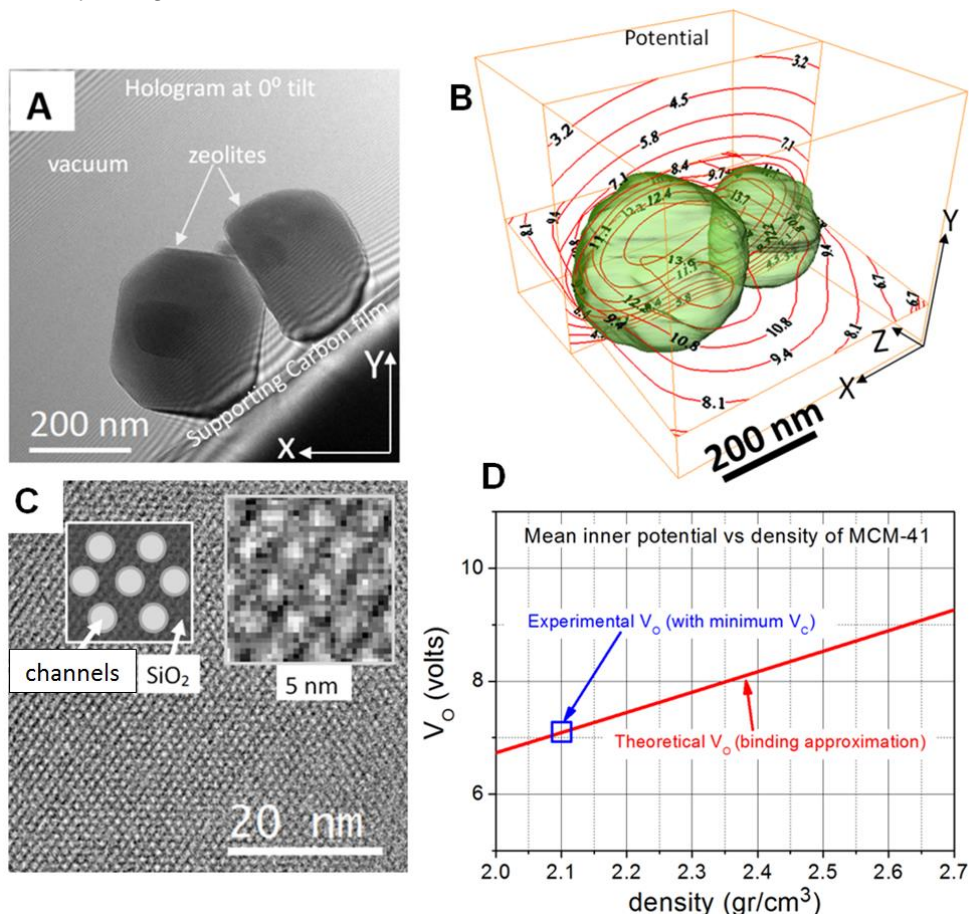


Figure 1. (A) Hologram of two MCM-41 zeolite nanoparticles acquired in a microscope FEGTEM Titan (B). Three-dimensional distribution of electrostatic potential (in Volts) inside and outside particles shown in (A) and measured using EHT. (C) Detail of the hexagonal structure of the zeolite with channels of 1 nm (B). (D) Theoretical values of the mean inner potential of the zeolites studied here using a binding approximation. The mean inner potential of the particles measured experimentally correspond approximately to an skeletal density of the zeolite of 2.1 gr/cm^3 .

References

- [1] A.C. Twitchett-Harrison, T.J.V. Yates, R.E. Dunin-Borkowski and P.A. Midgley, *Ultramicroscopy* 108 (2008) p. 1401.
- [2] R.E. Dunin-Borkowski, S.B. Newcomb, T. Kasama, M.R. McCartney, M. Weyland, P.A. Midgley, *Ultramicroscopy* 103 (2005) p. 67.
- [3] C.G. Sonwane et al. *J. Phys. Chem. B* 2005, 109, p. 23395.
- [4] M. Gajdardziska-Josifovska and A.H. Carim in "Applications of electron holography. In *Introduction to Electron Holography*", eds. L.F. Allard, D.C. Joy and E. Voelkl, (Plenum Press, New York) (1999), p. 267.
- [5] We kindly acknowledge for funding to the EC project REGPOT AL-NANOFUNC.

REMOTE PLASMA ASSISTED GLAD DEPOSITION OF OXIDE THIN FILM NANOSTRUCTURES FOR OPTICAL AND ELECTRONIC APPLICATIONS

Julián Parra-Barranco, Victor Rico, Ana Borrás, Juan Pedro Espinós, Fabián Frutos, Agustín R. González-Elipe, Ángel Barranco

Instituto de Ciencia de Materiales de Sevilla (ICMS), Centro Mixto CSIC-Universidad de Sevilla, Avda. Américo Vespucio 49, Isla de la Cartuja, 41092 Sevilla, Spain

julian.parra@icmse.csic.es

Abstract

Glancing angle deposited (GLAD) oxide thin films are quite interesting materials due to the possibilities on effective nanostructure control. Most important properties of the oxide GLAD thin films rely in the possibility to tailor the formation of tilted columns and other more complex forms and nanoporosity control. These nanostructures are caused by geometrical shadowing effects during the thin film growth. Porous GLAD films have been used as hosts or templates to fabricate different types of nanocomposite materials and other complex optical structures like photonic crystals, dye sensitized solar cells, optical sensors and microfluidic devices. [1-3]. In this work we study transparent and conducting Indium tin oxide films (ITO) by a novel synthetic approach consisting in GLAD deposition assisted by a microwave ECR plasma. The ECR microwave discharges are fully compatible with the range of pressures required for the electron evaporation process utilized for the deposition of the oxide thin films. The objective of the plasma discharge is to modify the growth mechanism of the GLAD process in order to introduce additional experimental parameters to control the columnar microstructure, porosity and other properties of the films. Thin films and multilayers synthesized in different plasma conditions and also in the presence of alternating plasma discharges will be studied. An additional advantage of the use of a plasma assisted process is the direct synthesis of oxide nanoporous thin films at near room temperature and the elimination/reduction of annealing processes required for final applications.

References

- [1] M. J. Brett and M. M. Hawkeye, *Science*, 319 (2008) 1192.
- [2] L. González-García, I. González-Valls, M. Lira-Cantu, A. Barranco and A.R. González-Elipe, *Energy and Environmental Science*, 4, (2011), 3426.
- [3] V. Rico, A. Borrás, F. Yubero, J.P Espinos, F. Frutos, A.R. Gonzalez-Elipe *J. Phys. Chem.* 113 (2009) 3775.

Quantification of InXGa1-xP Composition Modulation by Nanometric scale HAADF Simulations

C.E. Pastore ^{a*}, M. Gutiérrez ^a, D. Araújo ^a and E. Rodríguez-Messmer ^b

^a *Departamento de Ciencia de los Materiales e IM y QI, Universidad de Cádiz, 11510
Puerto Real, Spain.*

^b *Isofotón, C/ Severo Ochoa 50, 29590 Málaga, Spain*

*contact e-mail: carlo.pastore@uca.es

Keywords: electron microscopy; germanium; InGaP; semiconductor devices; phase separation.

Abstract

Multijunction III–V solar cells for terrestrial concentrator applications have attracted increasing attention in recent years for their very high conversion efficiencies, allowing dramatic reduction in the balance-of-system cost for photovoltaic electricity generation. Such multijunction cells use multiple subcell band gaps to divide the broad solar spectrum into smaller sections, each of which can be converted to electricity more efficiently[1].

The fundamental materials challenge is to approach optimal bandgaps while maintaining near-ideal materials quality. The highest conversion efficiency of solar cells has been achieved in stacked multijunction cells with three collecting cells of different band gaps. Recent progress based on three junction cells using GaInP /GaAs/Ge have been reported with conversion efficiencies above 40%[2,3]. However the epitaxial growth of III–V alloys entails other types of difficulties as disorder in alloy composition. In this sense, three situations are possible: (a) random distribution of atoms, (b) ordering and (c) composition modulation or phase separation. It is fundamental to control the semiconductor alloy composition since these properties affect device optoelectronic properties, as carrier mobility reduction and so its technological applications[4]. In this contribution we present a structural study of triple junction solar cell InGaP/InGaAs/Ge heterostructure grown on (0 0 1) germanium substrates to quantify the III-atom group composition variation of InGaP layer. Diffraction contrast mode of transmission electron microscopy (CTEM) allowed revealing the layer structure and composition modulation of InGaP layers with high sensitivity. To quantify the In-related variation, high angle annular dark field (HAADF) micrographs and profiles are compared to numerical simulated ones. The fit with the experimental contrast shows local variations of 4.25% In which should limit the cell efficiency.

- [1] J. M. Olson, S. R. Kurtz, A. E. Kibbler, and P. Faine, Appl. Phys. Lett. **56**, (1990) 623.
 [2] W. Guter, J. Schöne, S. P. Philipps, M. Steiner, G. Siefer, A. Wekkeli, E. Welsler, E. Oliva, A. W. Bett, and F. Dimroth, Appl. Phys. Lett. **94**, (2009). 223504.
 [3] R. R. King, D. C. Law, K. M. Edmondson, C. M. Fetzer, G. S. Kinsey, H. Yoon, R. A. Sherif, and N. H. Karam, Appl. Phys. Lett. **90**, (2007) 183516.
 [4] M. Gutiérrez, C. E. Pastore, D. Araújo, J. Miguel-Sánchez and E. Rodríguez-Messmer J.N.N. **10**, (2010)1.

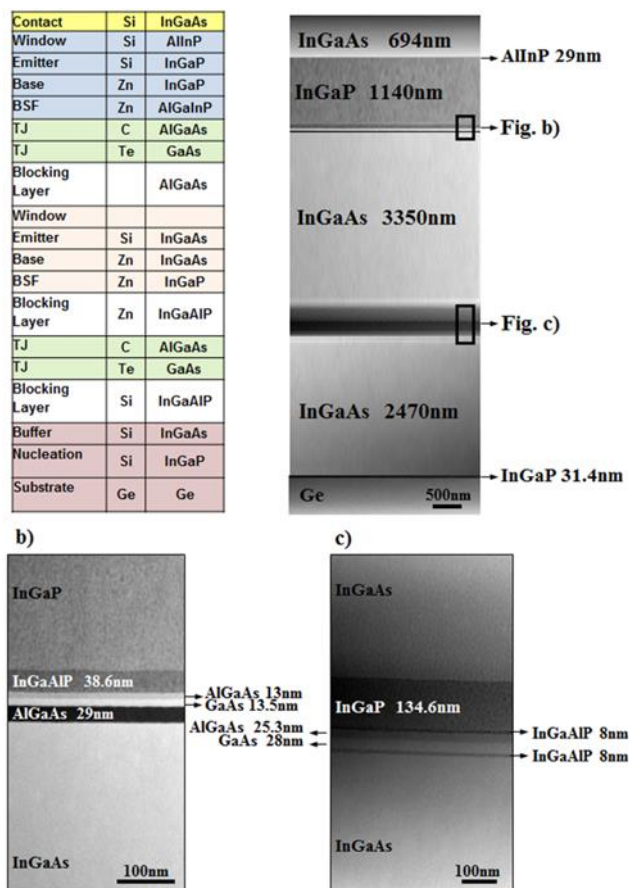


Fig.1: Schematic representation of the multijunction solar cell structure and the corresponding cross sectional view obtained by STEM-HAADF technique.

Characterization of amorphous porous Silicon coatings by Transmission Electron Microscopy techniques

Roland Schierholz^{a*}, Jaime Caballero^a, Vanda Godinho^a and Asunción Fernández^a

^a *Instituto de Ciencia de Materiales de Sevilla, Calle Américo Vespucio, 41092 Sevilla, España*

[*roland.schierholz@icmse.csic.es](mailto:roland.schierholz@icmse.csic.es)

Keywords: coatings, porous, TEM

Abstract

Amorphous Silicon coatings with closed porosity are produced by magnetron sputtering and characterized using transmission electron microscopy techniques to study the influence of deposition parameter on the microstructure.

The coatings are produced by glancing angle magnetron sputtering of Si targets in noble gas atmospheres. A similar process was previously applied to produce SiO_xN_y-coatings [1] which included pores filled with nitrogen. This time we use noble gases such as Helium and Argon in the atmosphere in the deposition process. Also we vary parameters such as pressure, flux, power mode of the magnetron, magnetron power, applied an additional bias as well as heating to the substrate. The changes in microstructure are then first studied by conventional transmission electron microscopy (TEM). Then selected samples are further studied by advanced TEM and scanning TEM (STEM) techniques. So energy filtered TEM (EFTEM) reveals that the additional peak at ≈ 10 eV in the plasmon range can be attributed to the pore matrix interface. Figure 1 shows two slices of an EFTEM spectrum image (SI) covering the low-loss region of a sample produced under Helium atmosphere. The spectrum extracted from position 2 only reveals the Silicon bulk plasmon located at 17 eV. The spectrum extracted from position 1 at the interface contains an additional peak producing a shoulder at ≈ 9 eV. The slice of the SI at 9 ± 2 eV reveals higher intensity at the surface of the closed pores.

The energy resolution of electron energy-loss spectroscopy (EELS) is higher in STEM-mode. In this mode we acquired spectra of the same sample in different points. The spectrum of a pore as shown in Figure 2 (a) reveals a signal of the Helium K-edge at 22 eV. The spectrum of the matrix in position 2 (Figure 2 (b)) only shows the Silicon bulk plasmon. By this technique we aim on quantification of He inside the pores as described by Walsh [2].

References

- [1] V. Godinho, C. Rojas and A. Fernandez, *Microporous and Mesoporous Materials*, **149** (2012) 142
- [2] C. A. Walsh, J. Yuan and L. M. Brown, *Philosophical Magazine A*, **80** (2000) 1507

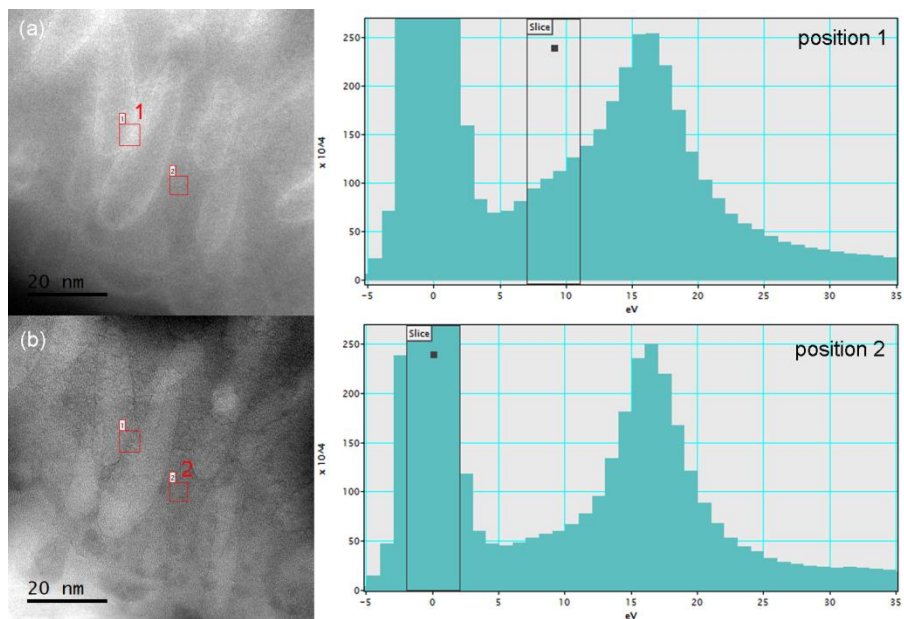


Figure 1 – EFTEM spectrum image of a porous Si-coating prepared under He-atmosphere. The slice at $9\pm 2\text{eV}$ (a) reveals the plasmon at the inner surface of the pores. The zero loss filtered image is shown in (b) as well as the spectrum at position 2, which reveals only the Si-plasmon. In contrast to this spectra extracted from position 1 at the pore wall reveals a shoulder at $\approx 9\text{ eV}$.

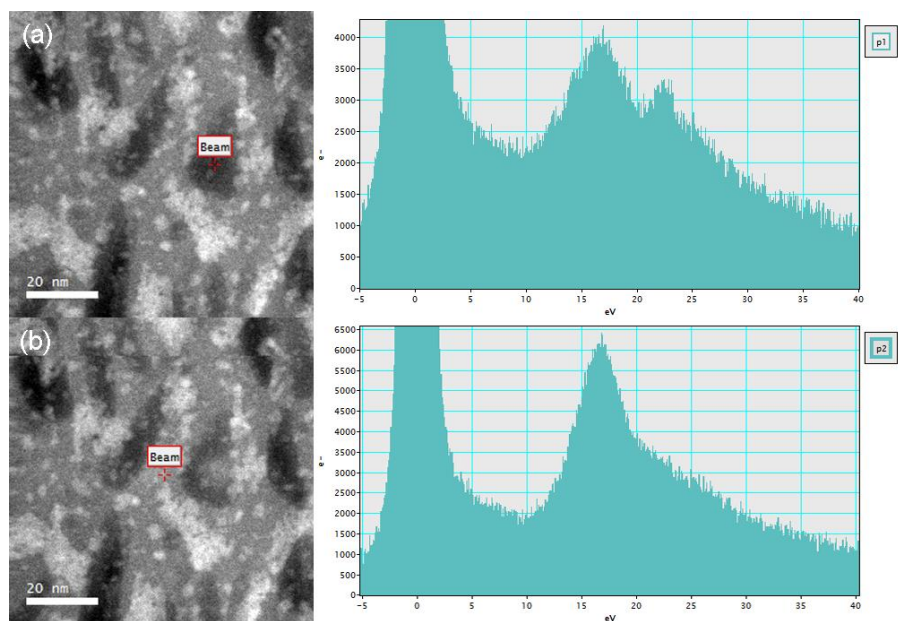


Figure 2 – STEM annular dark field images and EELS-spectra recorded at the two beam position p1 penetrating a pore and p2 only penetrating the matrix. The EELS spectrum of the pore shows a signal at 22 eV, the energy loss to excite the Helium K-edge. The bright spots in the STEM-image are contaminating particles due to ion milling.

Damage induced by rare earth ion implantation in nitride semiconductors: a comparative study

B. Lacroix^{a,*}, S. Jublot-Leclerc^b, A. Declémy^c, K. Lorenz^d, and P. Ruterana^a

^a CIMAP, 6, Bd Maréchal Juin, 14050 Caen, France

^b CSNSM, 91405 Orsay Campus, France

^c Institut Pprime, Bd Marie et Pierre Curie, 86962 Chasseneuil-Futuroscope, France

^d Instituto Tecnológico e Nuclear, Estrada Nacional 10, 2686-953 Sacavém, Portugal

*contact e-mail: bertrand.lacroix.bl.pro@gmail.com

Keywords: nitride semiconductors, rare earth implantation, damage mechanisms, stacking faults

Abstract

In recent years, rare earth doped III-V nitride semiconductors have received considerable attention for their promising applications in optoelectronics. In particular, due to the large band gaps of GaN and AlN that allow emission of high energy rare earth transitions, these materials have strong potentialities in the visible range with the development of the future multicolor devices [1] (full color displays, white light emitting diodes). In this scope, ion implantation is a very attractive technique, standard in the semiconductor technology for tuning the functionalities of materials by introducing dopants in selective areas with controllable concentrations and depths. However, this process also leads to damage that can degrade the material properties, and that thus needs to be subsequently annealed out.

In this work, we propose a comparative study of the damage formation in nitride semiconductors (GaN, AlN, InN) generated by 300 keV Eu implantation at RT in the $[10^{12} - 10^{17}]$ at./cm² fluence range. The damage mechanisms are investigated by combining transmission electron microscopy (TEM), X-ray diffraction (XRD) and Rutherford Backscattering Spectroscopy / Channeled (RBS/C) techniques.

In the case of InN, this investigation points out an extremely high sensitivity to ion beam damage and a fast degradation that starts from the lowest fluences (around 10^{12} at./cm²) [2]. Contrary to InN, GaN and AlN exhibit stronger resistance to the implantation damage and present similarities in the strain build-up. At low fluence, while RBS/C measurements remains insensitive to the implantation damage, a positive strain normal to the surface is measured by XRD, which steadily increases with the fluence. At higher fluences, the strain saturates in a localized region whilst it continues to strongly increase in another region of the material. In the same time, the damage level measured by RBS/C increases significantly, only in the bulk region in the case of AlN, whereas it takes place both in the bulk and at the surface of GaN. In light of TEM and HRTEM analysis, it is shown that the formation of basal and prismatic stacking faults plays a critical role in this damage formation in both materials [3-6]. The strain evolutions versus the implantation fluence are related to specific defective layers and are explained by different damage mechanisms (stacking faults formation and

extension, migration of point defects, and point defects clustering). In particular, the mechanisms that lead to the non-conventionnal nanocrystallization of the GaN surface around 2×10^{15} at./cm², not observed in the case of AlN, will be discussed.

References

- [1] A. J. Steckl and J. M. Zavada, *MRS Bulletin*, **24** (1999) 33.
- [2] B. Lacroix, M. P. Chauvat, P. Ruterana, K. Lorenz, E. Alves and A. Syrkin, *Journal of Physics D*, **44** (2011) 295402.
- [3] F. Gloux, T. Wojtowicz, P. Ruterana, K. Lorenz, and E. Alves, *Journal of Applied Physics*, **100** (2006) 073520.
- [4] P. Ruterana, B. Lacroix, and K. Lorenz, *Journal of Applied Physics*, **109** (2011), 013506.
- [5] B. Lacroix, S. Leclerc, A. Declémy, K. Lorenz, E. Alves and P. Ruterana, *Europhysics Letters*, **96** (2011) 46002.
- [6] S. Leclerc, B. Lacroix, A. Declémy, K. Lorenz, and P. Ruterana, *Journal of Applied Physics*, **112** (2012), 073525.

Relationship between morphological observations by transmission electron microscopy/X-Ray diffraction and physical properties of bio-based polymer/clay nanocomposites

Heriarivelo Risite^{a,b}, Omar Fassi-Fehri^{b,c}, Mostopha Bousmina^c, Khalil El Mabrouk^{a*}

^a MASCIR Foundation, Institute of Nanomaterials & Nanotechnology, ENSET, av. De l'Armée Royal, Madinat El Irfane 10100 – Rabat, Morocco

^b Faculté des Sciences, 4 av. Ibn Battouta B. P. 1014 – Rabat, Morocco

^c Hassan II Academy of Science and Technology Rabat, Morocco

*contact e-mail: k.elmabrouk@mascir.com

Abstract

In this study, we report the relationship between morphological observations by transmission electron microscopy (TEM), X-ray diffraction (XRD) and physical properties of polyamide 11/clay nanocomposites by the use of synthesized compatibilizer. XRD spectra of nanocomposites reveal that the increase of compatibilizing enhanced peak intensities observed at 5 wt % of clay loading indicating the reduction of stacks intercalated structure and leading to higher degree of delamination of clay. Mechanical behaviors improvement, suggested that the degree of dispersion of nanoclay within polymer matrix plays a vital role in property improvement. Detailed morphological studies and subsequent quantitative particles analyses for dispersed clay phase are still in measurement.

